

GALERKIN NEURAL NETWORKS: A FRAMEWORK FOR APPROXIMATING VARIATIONAL EQUATIONS WITH ERROR CONTROL

MARK AINSWORTH* AND JUSTIN DONG†

Abstract. We present a new approach to using neural networks to approximate the solutions of variational equations, based on the adaptive construction of a sequence of finite-dimensional subspaces whose basis functions are realizations of a sequence of neural networks. The finite-dimensional subspaces are then used to define a standard Galerkin approximation of the variational equation. This approach enjoys a number of advantages, including: the sequential nature of the algorithm offers a systematic approach to enhancing the accuracy of a given approximation; the sequential enhancements provide a useful indicator for the error that can be used as a criterion for terminating the sequential updates; the basic approach is largely oblivious to the nature of the partial differential equation under consideration; and, some basic theoretical results are presented regarding the convergence (or otherwise) of the method which are used to formulate basic guidelines for applying the method.

Key words. partial differential equations, a posteriori error estimate, neural networks

AMS subject classifications. 35A15, 65N38, 68T07

1 Introduction The current surge in interest in neural network approximation has witnessed the application of neural networks to a range of traditional problems in scientific computing and, in particular, the numerical solution of differential equations. The first problem encountered in applying neural networks to approximate the solution of a partial differential equation (PDE) is to decide on the basic formulation and how to choose the loss function to be used to train the network to approximate the true solution of the equation in hand. One popular formulation is to take the loss to be the square of the L^2 -norm of the residual in the equation augmented by additional terms to take account of the boundary conditions [1, 6, 16, 17, 21]. Similar approaches also form the basis for least squares type finite element methods, which are more mainstream approaches based on formulating the PDE and boundary conditions as a variational equation.

Variational approaches for constructing neural network approximations of PDEs have been explored in [11, 14, 23, 24]. While such approaches have enjoyed success in particular cases, in practice, the achievable relative error tends to stagnate around 0.1-1.0% irrespective of the number of neurons or layers used to define the underlying network architecture. In addition, despite recent progress [10, 19, 22], the current level of theoretical support and understanding of the behavior and convergence of neural network schemes pales in comparison to the vast literature on more traditional approaches. It seems that, at the time of writing, neural network methods are unable to offer a competitive alternative to more traditional approaches such as finite elements or spectral methods.

The current work follows a quite different approach to using neural networks to approximate variational equations, based on the adaptive construction of a sequence of finite-dimensional subspaces whose basis functions are realizations of a sequence of neural networks. The finite-dimensional subspaces can be used to define a standard

*Division of Applied Mathematics, Brown University (mark_ainsworth@brown.edu).

†Division of Applied Mathematics, Brown University (justin.dong@brown.edu).

Galerkin approximation of the variational equation. This approach enjoys a number of advantages: the need to train a single, large network is replaced by the solution of a sequence of smaller problems combined with a Galerkin approach to select the best linear combination of the resulting corrections; the sequential nature of the algorithm offers a systematic approach to enhancing the accuracy of a given approximation (without having to resort to training a new, larger network); the sequential enhancements can be shown to provide a useful indicator for the error in the current neural network approximation that can be used as a criterion for terminating the sequential updates; and the basic approach is to some extent oblivious to the nature of the PDE under consideration beyond assuming that a stable variational formulation is available. A notable feature of the approach is that it may be applied seamlessly to a broad class of problems including PDEs of various orders and spatial dimensions without major modifications. One may contrast this with more traditional approaches, such as finite element methods, which generally require significant structural modification if the spatial dimension or order of the PDE is changed. Finally, some basic theoretical results are presented regarding the convergence (or otherwise) of the method which are used to formulate some basic guidelines for applying the method.

The remainder of this paper is organized as follows. Section 2.1 summarizes some basic properties of Galerkin approximations that are needed in Section 2.2 where we describe a new approach for approximating the solutions of variational equations using neural networks. The main idea, developed in Section 2.3, is to adaptively construct a sequence of subspaces consisting of neural network functions from which a Galerkin approximation is obtained. Implementation details are provided in Section 2.4. The flexibility of the approach is illustrated in Section 3 by applying the method to approximate solutions of both second order and fourth order differential equations, including cases where the data and solutions are singular.

2 Basic Framework & Algorithm A feed-forward neural network with a single hidden layer of $n \in \mathbb{N}$ neurons defines a function $u_{NN} : \mathbb{R}^d \rightarrow \mathbb{R}$ as follows:

$$(2.1) \quad u_{NN}(x; \theta) = \sum_{j=1}^n c_j \sigma(x \cdot W_j + b_j), \quad x \in \Omega \subset \mathbb{R}^d,$$

where $d \in \mathbb{N}$ is fixed; Ω is a compact subset of \mathbb{R}^d ; $W_j \in \mathbb{R}^d$, $b_j \in \mathbb{R}$ are nonlinear parameters; $c_j \in \mathbb{R}$ are linear parameters; and $\sigma : \mathbb{R} \rightarrow \mathbb{R}$ is a smooth, bounded function. On occasion, we will use the shorthand notation $W = [W_1, \dots, W_n] \in \mathbb{R}^{d \times n}$, $b = [b_1, \dots, b_n] \in \mathbb{R}^{1 \times n}$, and $c = [c_1, \dots, c_n]^T \in \mathbb{R}^n$. In the standard nomenclature, n is referred to as the *width* of the network, W as the *weights*, b as the *biases*, and σ as the *activation function* of the hidden layer. The set of nonlinear and linear parameters is collectively denoted by $\theta = \{W, b, c\}$. The set of all functions of the form (2.1) is denoted by

$$(2.2) \quad V_n^\sigma := \{v : v(x) = \sum_{i=1}^n c_i \sigma(x \cdot W_i + b_i), \quad b_i, c_i \in \mathbb{R}, \quad W_i \in \mathbb{R}^d, \quad x \in \Omega\}.$$

We shall also define the subset of V_n^σ consisting of functions with bounded parameters. Given $C > 0$, we define

$$(2.3) \quad V_{n,C}^\sigma := \{v \in V_n^\sigma : \|\theta\| \leq C\},$$

where $\|\theta\| := \max_{ij} |W_{ij}| + \max_j |b_j| + \max_j |c_j|$.

Neural networks are known to be *universal approximators* [3,18] in the sense that the following result holds:

THEOREM 2.1. *Universal Approximation* [12]. *Suppose $1 \leq p < \infty$, $0 \leq s < \infty$, and $\Omega \subset \mathbb{R}^d$ is compact. If $\sigma \in C^s(\Omega)$ is nonconstant and bounded, then V_n^σ is dense in the Sobolev space*

$$W^{s,p}(\Omega) := \{v \in L^p(\Omega) : D^\alpha v \in L^p(\mu) \forall |\alpha| \leq s\}.$$

In particular, the universal approximation theorem means that given a function $f \in W^{s,p}(\Omega)$ and $\tau > 0$, there exists $n(\tau, f) \in \mathbb{N}$ and $\tilde{f} \in V_{n(\tau,f)}^\sigma$ such that $\|f - \tilde{f}\|_{W^{s,p}(\Omega)} < \tau$.

However, neural networks exhibit several undesirable properties as well. In particular, V_n^σ is not a vector space since it is not closed under addition. For instance, consider the case with $n = 1$ and $\sigma(t) = \max\{0, t\}$. Then $\sigma(t) \in V_1^\sigma$ and $\sigma(t-1) \in V_1^\sigma$, but $\sigma(t) + \sigma(t-1) \notin V_1^\sigma$. The fact that V_n^σ is not a vector space means we cannot draw upon many of the powerful results from functional analysis which are typically employed in analyzing the well-posedness of variational problems soon to be discussed. Moreover, V_n^σ is neither closed nor compact in $C(\Omega)$ or $L^p(\Omega)$. As demonstrated in [20] however, by restricting the network parameters as in $V_{n,C}^\sigma$, we can recover both closedness and compactness in $C(\Omega)$ and $L^p(\Omega)$. These topological properties of $V_{n,C}^\sigma$ become important in ensuring existence of a solution to the optimization problem we shall introduce in Section 2.2 (see Remark 2.4).

2.1 Galerkin Approximation of Variational Equations Let $s \in \mathbb{R}_{\geq 0}$ be fixed, let $X \subset H^s(\Omega) = W^{s,2}(\Omega)$ be a subspace with $V_n^\sigma \subset X$ a subset, and consider the variational equation: find

$$(2.4) \quad u \in X : \quad a(u, v) = L(v), \quad \forall v \in X,$$

where $L : X \rightarrow \mathbb{R}$ is a bounded linear operator and $a : X \times X \rightarrow \mathbb{R}$ is a bounded, symmetric, bilinear form on X satisfying the following condition:

$$(2.5) \quad a(v, v) \geq 0 \text{ with equality } \iff v = 0.$$

This condition implies that $a(\cdot, \cdot)$ defines an inner product on X and an associated norm given by $\|v\| := \sqrt{a(v, v)}$. In particular, the Cauchy-Schwarz inequality holds with respect to $\|\cdot\|$.

A standard application of the Riesz Representation Theorem [8] implies the existence of a unique $u \in X$ satisfying (2.4) with $\|u\| = \|L\|_*$, where $\|\cdot\|_*$ denotes the dual, or operator, norm of L given by

$$(2.6) \quad \|L\|_* := \sup_{v \in X \setminus \{0\}} \frac{|L(v)|}{\|v\|} = \sup_{v \in B} |L(v)|,$$

with $B = \{v \in X : \|v\| = 1\}$ being the unit sphere in X . As $X \subset H^s(\Omega)$, we observe that the universal approximation property holds for the norm $\|\cdot\|$ whenever $s \in \mathbb{N}$ [12]. That is, given $f \in X$ and $\tau > 0$, there exists $n(\tau, f) \in \mathbb{N}$ and $\tilde{f} \in V_{n(\tau,f)}^\sigma$ such that $\|f - \tilde{f}\| < \tau$. The result is extended to $s \in \mathbb{R}_{\geq 0}$ by the embedding $H^s(\Omega) \subset H^{\lfloor s \rfloor}(\Omega)$.

Remark 2.2. The width n of the network needed to ensure $\|f - \tilde{f}\| < \tau$ depends on both τ and f . For instance, suppose $f \in H^2(0, 1)$ and σ is chosen as the ReLU

function $t \mapsto \max\{0, t\}$. Standard results for piecewise linear approximation show that there exists a constant $\mathcal{C} > 0$ such that for all $m \in \mathbb{N}$, there exists $f_m \in V_m^\sigma$ satisfying $\|f - f_m\|_{L^2(0,1)} \leq \mathcal{C}m^{-2}\|f''\|_{L^2(0,1)}$. Hence, in order to achieve $\|f - f_m\|_{L^2(0,1)} < \tau$, it suffices to choose $m > \sqrt{\mathcal{C}\|f''\|_{L^2}/\tau}$. Observe that as the required tolerance decreases or the structure of f grows more complex, the width of the network needed to meet the tolerance will increase.

In general, the solution of the variational problem cannot be obtained in closed form and instead must be approximated. Given a finite-dimensional subspace $S \subset X$, the Galerkin approximation $u_S \in S$ of problem (2.4) consists of seeking

$$(2.7) \quad u_S \in S : \quad a(u_S, v_S) = L(v_S) \quad \forall v_S \in S.$$

Equally well, we have $u_S = P_S u$, where $P_S : X \rightarrow S$ is the orthogonal projection given by the rule $a(P_S z, v_S) = a(z, v_S)$, $\forall v_S \in S$ for each $z \in X$. Galerkin approximation schemes enjoy widespread usage due to the fact that they are not only stable since $\|P_S u\| \leq \|u\|$, but deliver the best approximation to the true solution u from the subspace S [2, 7], i.e.

$$(2.8) \quad \| \|u - u_S\| \| \leq \| \|u - v_S\| \|, \quad \forall v_S \in S.$$

Moreover, if $\{\varphi_j\}_{j=1}^m$ is a basis for S , then the approximation u_S may be computed explicitly by solving the linear system

$$(2.9) \quad \begin{cases} K \hat{u} = F \\ K_{ij} = a(\varphi_i, \varphi_j), \quad F_i = L(\varphi_i) \end{cases}$$

and forming $u_S = \sum_{j=1}^m \hat{u}_j \varphi_j$.

It is tempting to seek a neural network approximation $u_{NN} \approx u$ by employing a Galerkin scheme based on the choice $S = V_n^\sigma$. Unfortunately, the fact that V_n^σ is not a vector space nullifies much of the above discussion and precludes us from using it to define a Galerkin scheme of the form (2.7). Nonetheless, we observe that V_n^σ may still be utilized to generate approximations to u in two different ways.

First, by fixing the nonlinear parameters (W, b) and forming the subspace $\Phi := \text{span}\{\sigma(x \cdot W_i + b_i)\}_{i=1}^n$, a Galerkin approximation of the form (2.2) can be computed from Φ by choosing the linear parameters c as follows:

$$(2.10) \quad \begin{cases} Kc = F \\ K_{ij} = a(\sigma(x \cdot W_i + b_i), \sigma(x \cdot W_j + b_j)), \quad F_i = L(\sigma(w \cdot W_i + b_i)). \end{cases}$$

This process defines a function $c = \text{GALERKINLSQ}(W, b, \sigma, a, L)$ which computes the expansion coefficients of the projection of u onto the subspace $\Phi = \text{span}\{\sigma(x \cdot W_i + b_i)\}_{i=1}^n$ for fixed W and b . In practice, however, the freedom to vary W and b is largely responsible for the rich approximation power of neural networks. Nevertheless, the function GALERKINLSQ will play a role in Section 2.4.

Second, if $\{\psi_i\}_{i=1}^m$ is a linearly independent set of functions in V_n^σ , then we may similarly define $\Phi := \text{span}\{\psi_1, \dots, \psi_m\}$ and solve the linear system

$$(2.11) \quad \begin{cases} K \hat{u} = F \\ K_{ij} = a(\psi_i, \psi_j), \quad F_i = L(\psi_i) \end{cases}$$

from which the projection $P_\Phi u = \sum_{j=1}^m \hat{u}_j \psi_j$ may be obtained. This process defines a function $P_\Phi u = \text{GALERKINSOLVE}(\{\psi_1, \dots, \psi_m\}, a, L)$ which returns the projection of u onto the subspace $\Phi := \text{span}\{\psi_1, \dots, \psi_m\}$ with respect to the variational equation defined by the bilinear form a and data L . The routine `GALERKINSOLVE` will play a key role in Section 2.3.

2.2 Construction of the Galerkin Subspace Suppose $u_0 \in X$ is any given approximation to the solution of (2.4); even $u_0 = 0 \in X$ is allowed. Can we improve the accuracy of the approximation $u_0 \approx u$ by adding a suitable correction to u_0 from the set V_n^σ ?

We can measure how well u_0 approximates the true solution u by examining the residual $L(v) - a(u_0, v)$, $v \in X$ in (2.4), which vanishes if and only if $u_0 = u$. In general, the residual will be nonzero and defines a functional $r(u_0) : X \rightarrow \mathbb{R}$ given by the rule $\langle r(u_0), v \rangle = L(v) - a(u_0, v)$, where $\langle r(u_0), v \rangle$ denotes the duality pairing on X .

The following result establishes the relationship between the residual $r(u_0)$ and the error $u - u_0$ in the approximation $u \approx u_0$.

PROPOSITION 2.3. *Let $u_0 \in X$ be given and set $\varphi_1 := (u - u_0)/\|u - u_0\|$. Then $\langle r(u_0), \varphi_1 \rangle = \max_{v \in B} \langle r(u_0), v \rangle$, where B is the closed unit ball in X .*

Proof. Let $u_0 \in X$ be given. We use (2.4) to obtain

$$\langle r(u_0), v \rangle = L(v) - a(u_0, v) = a(u, v) - a(u_0, v) = a(u - u_0, v), \quad \forall v \in X.$$

By the Cauchy-Schwarz inequality,

$$\sup_{v \in B} \langle r(u_0), v \rangle = \sup_{v \in B} a(u - u_0, v) \leq \sup_{v \in B} \|u - u_0\| \cdot \|v\| = \|u - u_0\|.$$

On the other hand, choosing $v = \varphi_1 = (u - u_0)/\|u - u_0\| \in B$ yields

$$a(u_0 - u, v) = \frac{\|u - u_0\|^2}{\|u - u_0\|} = \|u - u_0\|,$$

and hence, $\max_{v \in B} \langle r(u_0), v \rangle = \|u - u_0\| = \langle r(u_0), \varphi_1 \rangle$. □

The elementary proof of Proposition 2.3 is illuminating in that it shows that the maximizer $\varphi_1 \in B$ of the residual is proportional to the error $e = u - u_0$. The optimal correction to u_0 is the true error e since $u_0 + e = u_0 + (u - u_0) = u$ yields the true solution. The fact that the maximizer φ_1 is proportional to the error means that we should take the correction to u_0 to be a multiple of φ_1 .

Unfortunately, we will not be able to compute the maximizer φ_1 explicitly which, as mentioned above, would be equivalent to solving the variational problem (2.4) exactly. Instead, we compute an approximation $\varphi_1^{NN} \approx \varphi_1$ by seeking

$$(2.12) \quad \varphi_1^{NN} \in V_{n,C}^\sigma : \langle r(u_0), \varphi_1^{NN} \rangle = \max_{v \in V_{n,C}^\sigma \cap B} \langle r(u_0), v \rangle.$$

Remark 2.4. A function φ_1^{NN} as defined in (2.12) exists. Observe that

$$\sup_{v \in V_{n,C}^\sigma \cap B} \langle r(u_0), v \rangle \leq \sup_{v \in B} \langle r(u_0), v \rangle < \infty.$$

Moreover, $V_{n,C}^\sigma$ is compact in $H^s(\Omega)$ by [20, Proposition 3.5] and thus, $V_{n,C}^\sigma \cap B$ is compact in X . The supremum is therefore achieved over $V_{n,C}^\sigma \cap B$ and, as a consequence, the function φ_1^{NN} appearing in (2.12) is well-defined.

We then form the subspace $S_1 = \text{span}\{\varphi_0^{NN}, \varphi_1^{NN}\}$ where $\varphi_0^{NN} := u_0/\|u_0\|$ and compute a Galerkin approximation to u by seeking

$$(2.13) \quad u_1 \in S_1 : a(u_1, v) = L(v) \quad \forall v \in S_1.$$

The following result demonstrates that if the network width n and the bound C are sufficiently large, then any such function $\varphi_1^{NN} \in V_{n,C}^\sigma$ as defined in (2.12) is a good approximation to φ_1 .

PROPOSITION 2.5. *Let $0 < \tau < 1$ be given. Then there exist $n(\tau, u_0) \in \mathbb{N}$ and $C(\tau, u_0) > 0$ such that if $n \geq n(\tau, u_0)$ and $C \geq C(\tau, u_0)$, then $\varphi_1^{NN} \in V_{n,C}^\sigma \cap B$ given by (2.12) satisfies $\|\varphi_1 - \varphi_1^{NN}\| < 2\tau/(1 - \tau)$.*

Proof. We first recall from Proposition 2.3 that

$$\varphi_1 = \arg \max_{v \in B} \langle r(u_0), v \rangle = \arg \max_{v \in B} a(u - u_0, v).$$

By the universal approximation property, there exists $n(\tau, u_0) \in \mathbb{N}$ and $\tilde{\varphi} \in V_n^\sigma$ such that $\|\varphi_1 - \tilde{\varphi}\| < \tau$. Furthermore, by the triangle inequality, we have $1 - \tau < \|\tilde{\varphi}\| < 1 + \tau$ or, equally well, $\|\tilde{\varphi}\| - 1 = \xi$ for some $\xi \in (-\tau, \tau)$. Let $\hat{\varphi} := \tilde{\varphi}/\|\tilde{\varphi}\| \in V_n^\sigma \cap B$. Then,

$$\begin{aligned} \|\varphi_1 - \hat{\varphi}\| &\leq \|\varphi_1 - \tilde{\varphi}\| + \|\tilde{\varphi} - \frac{1}{\|\tilde{\varphi}\|} \tilde{\varphi}\| \\ &< \tau + \frac{1}{\|\tilde{\varphi}\|} \|\|\tilde{\varphi}\| \cdot \tilde{\varphi} - \tilde{\varphi}\| \\ &< \tau + \frac{1}{1 - \tau} \|\|(1 + \xi)\tilde{\varphi} - \tilde{\varphi}\| \\ &= \tau + \frac{\xi}{1 - \tau} \|\tilde{\varphi}\| \\ &< \tau + \frac{\tau}{1 - \tau} (1 + \tau) = \frac{2\tau}{1 - \tau}. \end{aligned}$$

Set $C(\tau, u_0) := \|\hat{\theta}\|$, where $\hat{\theta}$ denotes the parameters corresponding to $\hat{\varphi} \in V_n^\sigma$.

Now, $\langle r(u_0), v \rangle = a(u - u_0, v) = \gamma a(\varphi_1, v)$ where $\gamma = \|u - u_0\|$. Let $n \geq n(\tau, u_0)$ and $C \geq C(\tau, u_0)$. The solution of (2.12) satisfies

$$\langle r(u_0), \varphi_1^{NN} \rangle = \max_{v \in V_{n,C}^\sigma \cap B} \langle r(u_0), v \rangle = \max_{v \in V_{n,C}^\sigma \cap B} \gamma a(\varphi_1, v).$$

Moreover, since $\gamma a(\varphi_1, v) \leq \gamma a(\varphi_1, \varphi_1^{NN})$ for all $v \in V_{n,C}^\sigma \cap B$,

$$\begin{aligned} \|\varphi_1 - \varphi_1^{NN}\|^2 &= \|\varphi_1\|^2 - 2a(\varphi_1, \varphi_1^{NN}) + \|\varphi_1^{NN}\|^2 \\ &= 2 - 2\gamma^{-1} \cdot \gamma a(\varphi_1, \varphi_1^{NN}) \\ &\leq 2 - 2\gamma^{-1} \cdot \gamma a(\varphi_1, \hat{\varphi}) \\ &= \|\varphi_1 - \hat{\varphi}\|^2 < 4\tau^2/(1 - \tau)^2 \end{aligned}$$

as required. \square

Proposition 2.5 shows that $\varphi_1^{NN} \in V_{n,C}^\sigma$ tends to the true maximizer φ_1 as the network width n increases. The next result shows that the corresponding approximation u_1 tends to the true solution u as n and C increase.

PROPOSITION 2.6. *Let $0 < \tau < 1$, $n(\tau, u_0) \in \mathbb{N}$, and $C(\tau, u_0)$ be as in Proposition 2.5, and u_1 be defined as in (2.13). Then $|||u - u_1||| \leq |||u - u_0||| \cdot \min\{1, 2\tau/(1 - \tau)\}$.*

Proof. Choosing $v_S = u_0 \in S_0$ in (2.8) yields $|||u - u_1||| \leq |||u - u_0|||$. Conversely, choosing $v_S = |||u_0||| \cdot \varphi_0^{NN} + |||u - u_0||| \cdot \varphi_1^{NN} \in S_0$ and recalling that $\varphi_1 = (u - u_0)/|||u - u_0|||$ yields

$$\begin{aligned} |||u - u_1||| &\leq |||(u - u_0) - |||u - u_0||| \cdot \varphi_1^{NN}||| \\ &= |||\varphi_1 \cdot |||u - u_0||| - |||u - u_0||| \cdot \varphi_1^{NN}||| \\ &= |||u - u_0||| \cdot |||\varphi_1 - \varphi_1^{NN}||| \\ &< |||u - u_0||| \cdot \frac{2\tau}{1 - \tau}, \end{aligned}$$

where the final step follows thanks to Proposition 2.5. \square

Proposition 2.6 gives a bound on the accuracy of the approximation $u \approx u_1$ in terms of τ and the (unknown) error in $u \approx u_0$. Interestingly, Proposition 2.3 shows that $|||u - u_0||| = \langle r(u_0), \varphi_1 \rangle$ which, were φ_1 available, would mean the actual error could be computed explicitly. Does replacing φ_1 by the approximation $\varphi_1 \approx \varphi_1^{NN}$ then result in a good estimator for the true error? To be precise, we define the quantity

$$(2.14) \quad \eta(u_0, v) := \langle r(u_0), v \rangle / |||v|||$$

and observe that $\eta(u_0, \varphi_1^{NN})$ can be evaluated explicitly once φ_1^{NN} and u_0 are in hand. The following result shows that, provided $\tau < 1/3$, the numerical value of $\eta(u_0, \varphi_1^{NN})$ is indeed equivalent to the true error $|||u - u_0|||$.

COROLLARY 2.7. *Let $\eta(u_0, v)$ be as defined in (2.14). If $0 < \tau < 1/3$, then*

$$(2.15) \quad \frac{1 - \tau}{1 + \tau} \eta(u_0, \varphi_1^{NN}) \leq |||u - u_0||| \leq \frac{1 - \tau}{1 - 3\tau} \eta(u_0, \varphi_1^{NN}).$$

Proof. By Proposition 2.3, we have $|||u - u_0||| = \langle r(u_0), \varphi_1 \rangle$. Hence,

$$|\eta(u_0, \varphi_1^{NN}) - |||u - u_0||| | = |\langle r(u_0), \varphi_1^{NN} \rangle - \langle r(u_0), \varphi_1 \rangle| = |a(u - u_0, \varphi_1^{NN} - \varphi_1)|,$$

and applying Proposition 2.5 yields

$$|\eta(u_0, \varphi_1^{NN}) - |||u - u_0||| | \leq |||u - u_0||| \cdot |||\varphi_1^{NN} - \varphi_1||| < |||u - u_0||| \cdot \frac{2\tau}{1 - \tau}.$$

If $\tau \in (0, 1/3)$ then $2\tau/(1 - \tau) \in (0, 1)$, and hence

$$\eta(u_0, \varphi_1^{NN}) \leq |||u - u_0||| \cdot \left(\frac{2\tau}{1 - \tau} + 1 \right) = |||u - u_0||| \cdot \frac{1 + \tau}{1 - \tau}$$

and

$$\eta(u_0, \varphi_1^{NN}) \geq |||u - u_0||| \cdot \left(-\frac{2\tau}{1 - \tau} + 1 \right) = |||u - u_0||| \cdot \frac{1 - 3\tau}{1 - \tau}.$$

Combining these estimates gives (2.15). \square

In summary, once the solution φ_1^{NN} of (2.12) is in hand, we can (a) obtain an improved approximation to $u \approx u_1$ by solving (2.13) and (b) obtain a numerical estimate $\eta(u_0, \varphi_1^{NN}) \approx |||u - u_0|||$ for the error. The foregoing arguments show that if $\tau \rightarrow 0$, or, equally well, the network width $n \rightarrow \infty$ and bound $C \rightarrow \infty$, then the resulting approximation $u_1 \rightarrow u$ (in X) and $\eta(u_0, \varphi_1^{NN}) \rightarrow |||u - u_0|||$ (in \mathbb{R}).

2.3 Galerkin Subspace Augmentation The procedure outlined in the preceding section gives an improved approximation $u_1 = P_{S_1}u$ to u from the two-dimensional subspace $S_1 = \text{span}\{\varphi_0^{NN}, \varphi_1^{NN}\}$. How should we proceed if the approximation $u \approx u_1$ is lacking? A natural extension of this approach would be to apply the same procedure that was used to improve the approximation $u \approx u_0$ to improve u_1 . Namely, we compute an approximate maximizer φ_2^{NN} of the new residual $\langle r(u_1), v \rangle$ and use it to further augment the Galerkin subspace by setting $S_2 = \text{span}\{\varphi_0^{NN}, \varphi_1^{NN}, \varphi_2^{NN}\}$. Proceeding recursively, we construct the finite-dimensional subspace $S_j = \text{span}\{\varphi_0^{NN}, \varphi_1^{NN}, \varphi_2^{NN}, \dots, \varphi_j^{NN}\}$ with $\varphi_i^{NN} \in V_{n_i, C_i}^{\sigma_i}$.

Here, we have allowed for the possibility to vary both the network width n_i and activation function σ_i . Proceeding as in Section 2.2, we define $\varphi_i = (u - u_{i-1})/\|u - u_{i-1}\|$ and compute an approximation to φ_i by seeking

$$(2.16) \quad \varphi_i^{NN} \in V_{n_i, C_i}^{\sigma_i} : \langle r(u_{i-1}), \varphi_i^{NN} \rangle = \max_{v \in V_{n_i, C_i}^{\sigma_i} \cap B} \langle r(u_{i-1}), v \rangle$$

and then computing a new approximation $u \approx u_i$ as follows:

$$(2.17) \quad u_i \in S_i : a(u_i, v) = L(v) \quad \forall v \in S_i,$$

or, equally well, $u_i = P_{S_i}u$.

We have the following analogs to Propositions 2.3, 2.5, and 2.6 and Corollary 2.7.

COROLLARY 2.8. *For each $i > 0$, let $u_i = P_{S_i}u$ be given and define $\varphi_i := (u - u_{i-1})/\|u - u_{i-1}\|$. Then $\langle r(u_{i-1}), \varphi_i \rangle = \max_{v \in B} \langle r(u_{i-1}), v \rangle$.*

COROLLARY 2.9. *For each $i > 0$, let $0 < \tau_i < 1$ be given. Then there exists $n(\tau_i, u_{i-1}) \in \mathbb{N}$ and $C(\tau_i, u_{i-1}) > 0$ such that if $n \geq n(\tau_i, u_{i-1})$ and $C \geq C(\tau_i, u_{i-1})$, then the function $\varphi_i^{NN} \in V_{n, C}^{\sigma_i}$ as defined in (2.16) satisfies $\|\varphi_i - \varphi_i^{NN}\| < 2\tau_i/(1 - \tau_i)$. Moreover, if $\tau_i < 1/3$, then*

$$\frac{1 - \tau_i}{1 + \tau_i} \eta(u_{i-1}, \varphi_i^{NN}) \leq \|u - u_{i-1}\| \leq \frac{1 - \tau_i}{1 - 3\tau_i} \eta(u_{i-1}, \varphi_i^{NN}).$$

In particular, Corollary 2.9 provides a computable estimate of the error $\|u - u_{i-1}\|$ that can be used as a stopping criterion for the recursive solution procedure as follows: Given a tolerance $\text{tol} > 0$, if $\eta(u_{i-1}, \varphi_i^{NN}) > \text{tol}$, then we augment the subspace S_{i-1} to $S_i = S_{i-1} \oplus \{\varphi_i^{NN}\}$ and compute an updated approximation $u_i \approx u$; otherwise, the approximation u_{i-1} is deemed satisfactory, and the procedure terminates. Algorithm 1 summarizes this recursive approach, where the function AUGMENTBASIS is the routine which computes the maximizer φ_i^{NN} in the subspace augmentation process and which will be described in Section 2.4.

The next result addresses the convergence, or otherwise, of the recursive procedure.

COROLLARY 2.10. *Let $j \geq 1$. If $\{\tau_i\}_{i=1}^j$, $\{n(\tau_i, u_{i-1})\}_{i=1}^j$, and $\{C(\tau_i, u_{i-1})\}_{i=1}^j$ are chosen as in Corollary 2.9, then*

$$\|u - u_j\| \leq \|u - u_0\| \cdot \prod_{i=1}^j \min\left\{1, \frac{2\tau_i}{1 - \tau_i}\right\}.$$

Proof. Proposition 2.6 implies that for each i : $\|u - u_i\| \leq \|u - u_{i-1}\| \cdot \min\{1, 2\tau_i/(1 - \tau_i)\}$. Bootstrapping this result gives

$$\|u - u_j\| \leq \|u - u_{j-1}\| \cdot \min\left\{1, \frac{2\tau_j}{1 - \tau_j}\right\}$$

Algorithm 1: Adaptive Construction of Subspace.

Input: Data L , bilinear operator a , network widths $\{n_i\}$, initial approximation $u_0 \in X$, tolerance $\mathbf{tol} > 0$.

Output: Stopping iteration $N \in \mathbb{N}$, numerical approximation u_N to the variational problem: $u \in X$ such that $a(u, v) = \langle f, v \rangle$ for all $v \in X$; basis functions $\{\varphi_i^{NN}\}_{i=0}^N$.

1 **Require:**

2 a symmetric and $a(v, v) \geq 0$, with $a(v, v) = 0$ if and only if $v = 0$.

3 Set $i = 1$ and $\varphi_0^{NN} = u_0 / \|u_0\|$.

4 $(\varphi_1^{NN}, \eta) \leftarrow \text{AUGMENTBASIS}(u_0)$.

5 **while** $\eta > \mathbf{tol}$ **do**

6 $u_i \leftarrow \text{GALERKINSOLVE}(\{\varphi_0^{NN}, \varphi_1^{NN}, \dots, \varphi_i^{NN}\}, a, L)$

7 $(\varphi_{i+1}^{NN}, \eta) \leftarrow \text{AUGMENTBASIS}(u_i)$.

8 Set $i \leftarrow i + 1$.

9 **end**

10 Return $N = i - 1$, u_N , and $\{\varphi_j^{NN}\}_{j=0}^N$.

$$\begin{aligned} & \vdots \\ & \leq \|u - u_0\| \cdot \prod_{i=1}^j \min\left\{1, \frac{2\tau_i}{1 - \tau_i}\right\} \end{aligned}$$

as claimed. \square

Lastly, we discuss the conditioning of the linear system $K^{(j)}\hat{u} = F^{(j)}$ associated with the approximation $u \approx u_j$ in (2.17). This linear system follows the framework described by (2.11). The matrix $K^{(j)}$ has entries

$$K_{k\ell}^{(j)} = a(\varphi_{k-1}^{NN}, \varphi_{\ell-1}^{NN}),$$

where the basis functions $\{\varphi_i^{NN}\}_{i=0}^j$ are obtained according to Algorithm 1. We observe that if $k = \ell$, then $K_{kk}^{(j)} = 1$ since $\varphi_k^{NN} \in B$.

PROPOSITION 2.11. *Let $\{\varphi_i^{NN}\}_{i=0}^N$ be the set of basis functions constructed by Algorithm 1. Then for $i > 1$, $\varphi_i^{NN} \notin S_{i-1}$. Moreover, if $\gamma = \sum_{k=1}^N 2\tau_k / (1 - \tau_k) < 1$, then*

$$(2.18) \quad \text{cond}(K^{(N)}) < \frac{1 + \gamma}{1 - \gamma}.$$

Proof. Suppose, to the contrary, that $\varphi_i^{NN} \in S_{i-1}$. Then (2.17) implies $L(\varphi_i^{NN}) - a(u_{i-1}, \varphi_i^{NN}) = \eta(u_{i-1}, \varphi_i^{NN}) = 0$. But the stopping criterion in Algorithm 1 (see Line 5) ensures that each φ_i^{NN} satisfies $\eta(u_{i-1}, \varphi_i^{NN}) > \mathbf{tol}$, a contradiction. Thus, $\varphi_i^{NN} \notin S_{i-1}$ and, in particular, the functions $\{\varphi_i^{NN}\}_{i=0}^N$ are linearly independent.

For the second assertion, if $k > \ell$, then we have $a(\varphi_k, \varphi_\ell^{NN}) \propto a(u - u_{k-1}, \varphi_\ell^{NN}) = 0$ by (2.17), and applying Corollary 2.9 yields

$$|a(\varphi_k^{NN}, \varphi_\ell^{NN})| = |a(\varphi_k^{NN}, \varphi_\ell^{NN}) - a(\varphi_k, \varphi_\ell^{NN})| = |a(\varphi_k^{NN} - \varphi_k, \varphi_\ell^{NN})|$$

$$\leq |||\varphi_k^{NN} - \varphi_k||| \cdot |||\varphi_\ell^{NN}||| < \frac{2\tau_k}{1 - \tau_k}.$$

Thus, $|K_{\ell k}^{(N)}| = |K_{k\ell}^{(N)}| < 2\tau_\ell/(1 - \tau_\ell)$ for $k \neq \ell$ thanks to the symmetry of $a(\cdot, \cdot)$.

By Gershgorin's Theorem [9], for each eigenvalue λ of $K^{(N)}$ there exists ℓ such that

$$|\lambda - K_{\ell\ell}^{(N)}| = |\lambda - 1| < \sum_{k \neq \ell} |K_{k\ell}^{(N)}| < \sum_{k \neq \ell} \frac{2\tau_k}{1 - \tau_k}.$$

Then $|\lambda - 1| < \gamma$ for each λ , and

$$\text{cond}(K^{(N)}) = \frac{|\max \lambda|}{|\min \lambda|} < \frac{1 + \gamma}{1 - \gamma}$$

as claimed. \square

In summary, the procedure given by Algorithm 1 adaptively constructs a subspace using the basis functions $\varphi_i^{NN} \in V_{n_i, C_i}^{\sigma_i}$, $i = 1, \dots, N$. By Corollary 2.10, the resulting Galerkin approximation u_N converges to u provided that the widths n_i and bounds C_i are sufficiently large. Moreover, the off-diagonal entries of $K^{(N)}$ are small provided that n_i and C_i are sufficiently large. In particular, $\text{cond}(K^{(N)}) \approx 1$.

2.3.1 Selection of Network Widths Algorithm 1 allows for the flexibility to vary both the width n_i of the network and the activation function σ_i as i is increased. Surprisingly, we can fix n and set $n_i \equiv n$ and yet still hope to achieve convergence as $i \rightarrow \infty$:

PROPOSITION 2.12. *Let $n \in \mathbb{N}$ be fixed and $\Omega \subset \mathbb{R}^d$ compact. Suppose $f \in H^s(\Omega)$, $s \in \mathbb{R}_{\geq 0}$. For $\tau > 0$, there exists $r \in \mathbb{N}$ and $\{u_j\}_{j=1}^r \in V_n^\sigma$ such that $\|f - \sum_{j=1}^r u_j\|_{H^s} < \tau$.*

Proof. By the universal approximation property, there exists $n(\tau, f) \in \mathbb{N}$ and $\hat{f} \in V_{n(\tau, f)}^\sigma$ such that $\|f - \hat{f}\|_{H^s} < \tau$. Choose r such that $rn > n(\tau, f)$. Then there exists $\tilde{f} \in V_{nr}^\sigma$ such that $\|f - \tilde{f}\|_{H^s} < \tau$, where $\tilde{f}(x) = \sum_{k=1}^{nr} c_k \sigma(x \cdot W_k + b_k) = \sum_{j=1}^r u_j(x)$, with $u_j(x) = \sum_{k > (j-1)n}^{jn} c_k \sigma(x \cdot W_k + b_k)$. \square

Proposition 2.12 shows that any $f \in H^s(\Omega)$ can be approximated by a sum of functions in V_n^σ to arbitrary accuracy. In principle, this means fixing $n_i \equiv n$ and carrying out sufficiently many iterations of Algorithm 1 should give convergence. However, in practice the rate of convergence will become arbitrarily slow.

For instance, let us again consider the scenario described in Remark 2.2, where it was found that a ReLU network of width $n(\tau, f) = \sqrt{C \|f''\|_{L^2}/\tau}$ was sufficient to approximate a function $f \in H^2(0, 1)$ to a tolerance τ in $L^2(0, 1)$. The proof of Proposition 2.12 shows that a sum of $r \geq n^{-1} \sqrt{C \|f''\|_{L^2}/\tau}$ functions in V_n^σ achieves a tolerance of τ . In other words, $\mathcal{O}(\tau^{-1/2})$ iterations of Algorithm 1 are needed to achieve tolerance τ . This means that, on average, the error is reduced by a factor of $\tau^{\sqrt{\tau}}$ per iteration of the algorithm during this phase. However, in the limit as $\tau \rightarrow 0$, the average reduction factor tends to 1, i.e. the algorithm converges arbitrarily slowly.

A similar conclusion is reached if one considers Corollary 2.10 with $n_i = n$ is fixed. Specifically, the sequence $\{\tau_i\}_{i=1}^j$ will generally be increasing due to the decreased ability of a fixed-width network $\varphi_i^{NN} \in V_{n, C}^\sigma$ to capture higher resolution features of the error as i increases. In other words, there exists $i^* \in \mathbb{N}$ such that $\min\{1, 2\tau_i/(1 - \tau_i)\} = 1$ for all $i \geq i^*$, meaning that the convergence stagnates eventually.

On the other hand, Corollary 2.10 also suggests how we might avoid this stagnation. Observe that if $0 < \tau < 1/3$ is fixed and $\tau_i = \tau$ for all i , then it is expected that the sequence $\{n(\tau, u_i)\}_{i=0}^j$ is nondecreasing. In particular, the error in u_i is a factor of $2\tau/(1-\tau)$ smaller than the error in u_{i-1} . In order for $\varphi_i^{NN} \in V_{n(\tau, u_{i-1}), C(\tau, u_{i-1})}^{\sigma_i}$ to capture the higher resolution features of $(u - u_{i-1})/\|u - u_{i-1}\|$ (as compared to the relatively lower resolution features of $(u - u_{i-2})/\|u - u_{i-2}\|$), we necessarily require that $n(\tau, u_{i-1}) > n(\tau, u_{i-2})$. Hence, by increasing the width n_i of the networks as i increases, we have $\|u - u_j\| \leq \|u - u_0\| \cdot (2\tau/(1-\tau))^j$.

2.4 Neural Network Approximation of Augmented Basis Function In order to compute the augmented basis function $\varphi_i^{NN} \in V_{n_i, C_i}^{\sigma_i} \cap B$ according to (2.16), we first note that functions $v \in V_{n_i, C_i}^{\sigma_i}$ do not necessarily satisfy $\|v\| = 1$. We thus normalize by forming $v/\|v\|$:

$$(2.19) \quad \max_{v \in V_{n_i, C_i}^{\sigma_i} \cap B} \langle r(u_{i-1}), v \rangle = \max_{v \in V_{n_i, C_i}^{\sigma_i} \setminus \{0\}} \langle r(u_{i-1}), \frac{v}{\|v\|} \rangle = \max_{v \in V_{n_i, C_i}^{\sigma_i} \setminus \{0\}} \eta(u_{i-1}, v),$$

where $\eta(u_{i-1}, v)$ is as defined in (2.14). Next, we note that any $v \in V_{n_i, C_i}^{\sigma_i}$ is fully characterized by the set of parameters $\theta^{(i)} = (W^{(i)}, b^{(i)}, c^{(i)})$. Thus, (2.19) becomes

$$(2.20) \quad \max_{v \in V_{n_i, C_i}^{\sigma_i} \setminus \{0\}} \eta(u_{i-1}, v) = \max_{\substack{\theta^{(i)} \\ \theta \neq (0,0,0) \\ \|\theta^{(i)}\| < C_i}} \eta(u_{i-1}, v(\theta^{(i)})).$$

In practice, we do not enforce boundedness of $\theta^{(i)}$. While boundedness can be enforced by selecting a large value of C_i and clipping the network parameters should they exceed this value during training, we find that for the examples in Section 3, the network parameters are uniformly bounded without explicitly enforcing $\|\theta^{(i)}\| < C_i$.

The standard approach to computing optima of objective functions associated with neural networks is to apply a gradient-based optimizer to all of the parameters in θ , for example [1, 6, 14, 16, 21, 23, 24]. In order to solve (2.16), we instead propose a training procedure in the spirit of [4] as follows:

1. On the first training iteration, the hidden parameters $(W^{(i)}, b^{(i)})$ are initialized appropriately, which we describe on a case-by-case basis in Section 3. Otherwise, the hidden parameters are updated via a gradient-based optimizer. For instance, with gradient descent, the update is described by

$$(2.21) \quad W^{(i)} \leftarrow W^{(i)} + \alpha \nabla_{W^{(i)}} \left[\eta(u_{i-1}, v(\theta^{(i)})) \right]$$

$$(2.22) \quad b^{(i)} \leftarrow b^{(i)} + \alpha \nabla_{b^{(i)}} \left[\eta(u_{i-1}, v(\theta^{(i)})) \right]$$

with learning rate α .

2. We form $\Phi := \text{span}\{\sigma(x \cdot W_j + b_j)\}_{j=1}^n$ and take the projection $v(\theta^{(i)}) \leftarrow P_{\Phi}(u - u_{i-1})$ as described by GALERKINLSQ($W^{(i)}, b^{(i)}, \sigma_i, a, L(\cdot) - a(u_{i-1}, \cdot)$). The solution of the linear system (2.10) with the data $L(\cdot) - a(u_{i-1}, \cdot)$ provides the expansion coefficients of the projection of the error $u - u_{i-1}$ onto Φ with respect to a . Specifically, by (2.8), $P_{\Phi}(u - u_{i-1})$ is the best approximation to $u - u_{i-1}$ from Φ .

The training procedure for φ_i^{NN} is summarized in Algorithm 2.

¹We use a number of existing initializations for the hidden parameters in our examples, which are detailed in Section 3.

Algorithm 2: Basis Function Generation and Error Estimation.

Input: Data L , bilinear operator a , network width n_i , activation function σ_i , initial approximation $u_{i-1} \in X$.

Output: Numerical approximation φ_i^{NN} to the maximizer $\arg \max_{v \in B} \langle r(u_i), v \rangle = (u - u_{i-1}) / \|u - u_{i-1}\|$, and error estimator $\eta(u_{i-1}, \varphi_i^{NN}) \approx (u - u_{i-1}) / \|u - u_{i-1}\|$

- 1 **Function AugmentBasis**(u_j):
- 2 Initialize hidden parameters $(W^{(i)}, b^{(i)}) \in \mathbb{R}^{d \times n_i} \times \mathbb{R}^{n_i}$.
- 3 Compute corresponding activation coefficients:
 $c^{(i)} \leftarrow \text{GALERKINLSQ}(W^{(i)}, b^{(i)}, \sigma_i, a, L(\cdot) - a(u_{i-1}, \cdot))$.
- 4 **for each training epoch do**
- 5 Compute the update rule for $(W^{(i)}, b^{(i)})$:

$$W^{(i)} \leftarrow W^{(i)} + \alpha \nabla_{W^{(i)}} \left[\eta(u_{i-1}, v(\theta^{(i)})) \right]$$

$$b^{(i)} \leftarrow b^{(i)} + \alpha \nabla_{b^{(i)}} \left[\eta(u_{i-1}, v(\theta^{(i)})) \right].$$
- Compute corresponding activation coefficients:
 $c^{(i)} \leftarrow \text{GALERKINLSQ}(W^{(i)}, b^{(i)}, \sigma_i, a, L(\cdot) - a(u_{i-1}, \cdot))$.
- 6 **end**
- 7 Return $\varphi_i^{NN} = v(\theta^{(i)}) / \|v(\theta^{(i)})\|$ and $\eta(u_{i-1}, \varphi_i^{NN})$.
- 8 **EndFunction**

2.4.1 Implementation Details Most problems in which the bilinear operator a is associated with the weak formulation of a PDE require the computation of L^2 inner products in Ω . For instance, consider the case with $a(u, v) := (u, v)_{L^2(\Omega)}$ and $L(v) := (f, v)_{L^2(\Omega)}$ where $f \in L^2(\Omega)$. In order to compute the objective function $\eta(u_0, v(\theta)) = \langle r(u_0), v(\theta) \rangle / \|v(\theta)\|$, we approximate the associated integrals by employing a quadrature rule consisting of nodes $\{x_i\}_{i=1}^{n_G} \subset \Omega$ and weights $\{w_i\}_{i=1}^{n_G}$:

$$\int_{\Omega} v(x) dx \approx \sum_{i=1}^{n_G} w_i v(x_i).$$

We refer the reader to [5] for further details on the derivation, accuracy, and convergence of such quadrature rules.

The objective function in the above example is approximated by

$$\frac{L(v(\theta)) - a(u_0, v(\theta))}{\|v(\theta)\|} \approx \frac{\sum_{i=1}^{n_G} w_i [f(x_i)v(x_i; \theta) - u_0(x_i)v(x_i; \theta)]}{\sqrt{\sum_{i=1}^{n_G} w_i v(x_i; \theta)^2}}.$$

In all examples in Section 3, a single step of the Adam optimizer [15] with full batch is employed to update the hidden parameters $\{W, b\}$ at each training epoch following Algorithm 1. In other words, the training data essentially consists of the set of n_G quadrature nodes which are used to evaluate the loss function.

For most numerical examples, the activation function σ_i at Galerkin iteration i is adaptive in the sense that we utilize a scaling factor as a hyperparameter [13]. Given a fixed nonpolynomial activation function $\sigma : \mathbb{R} \rightarrow \mathbb{R}$, we define $\sigma_i(t) = \sigma(\beta_i t)$,

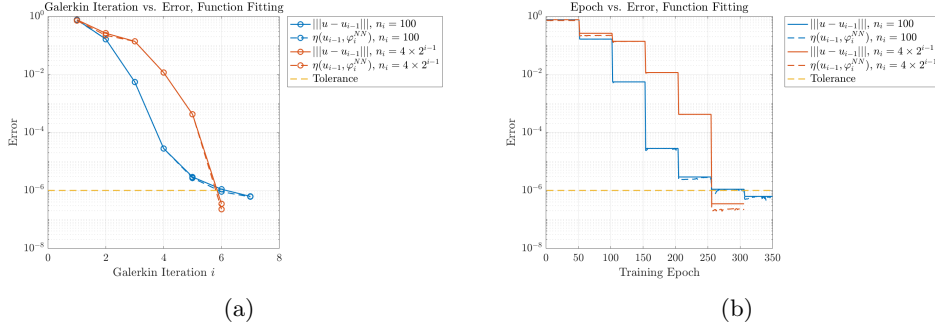


Fig. 1: (a) Estimated and true L^2 error at each Galerkin iteration. (b) The piecewise constant segments (solid lines) denote the true errors for each Galerkin iteration i , while the dashed red line (resp. blue line) denotes the progress of the loss function in approximating the true errors within each Galerkin iteration for increasing network widths (resp. constant network widths). The x -axis thus denotes the cumulative training epoch over all Galerkin iterations.

where $\{\beta_i\}$ is a nondecreasing sequence in \mathbb{R}_+ . As β_i grows larger, the gradient of σ_i generally increases, which allows for better resolution of the fine-scale error features as we shall demonstrate in Section 3. Finally, in most of the proceeding examples, the network widths $\{n_i\}$ follow a geometric progression of the form $n_i = N \cdot r^{i-1}$, where N is the initial width for the first Galerkin iteration r is the geometric ratio. The learning rate is fixed for each Galerkin iteration i and follows an exponential decay of the form $\alpha_i = A \cdot \rho^{-(i-1)}$, where A is the initial learning rate for the first Galerkin iteration and ρ is the rate of decay. Standard neural network approaches where one trains only a single fixed-architecture network commonly utilize a decreasing learning rate schedule as the training epochs progress. In our approach, we only decrease the learning rate *between* each Galerkin iteration to compensate for the increasing widths n_i as described in Section 2.3.1.

The main computational expense in Algorithm 1 is the computation of the activation coefficients c_j defined by the dense linear system (2.10) which costs $\mathcal{O}(n_i^3)$ operations for Galerkin iteration i . If the network size n_0 is increased by a fixed factor $\mu > 1$ at each iteration, then the total computational cost is of order

$$\sum_{i=1}^k \mu^{3(i-1)} n_0^3 = n_0^3 \frac{\mu^{3k} - 1}{\mu^3 - 1} \approx n_F^3,$$

where $n_F = n_0 \mu^{k-1}$ is the number of neurons in the final network. In other words, the computational cost associated with obtaining c for the entire sequence of networks is comparable to the cost of a single network of width n_F .

3 Applications We apply Algorithm 1 to a number of problems in one and two dimensions, demonstrating the robustness of our algorithm for several different classes of problems as well as the robustness of the error indicator $\eta(u_{i-1}, \varphi_i^{NN})$.

3.1 Function Fitting We consider the following illuminating example in order to investigate whether stagnation of the error $\|u - u_i\|$ occurs when $n_i \equiv n$ is fixed:

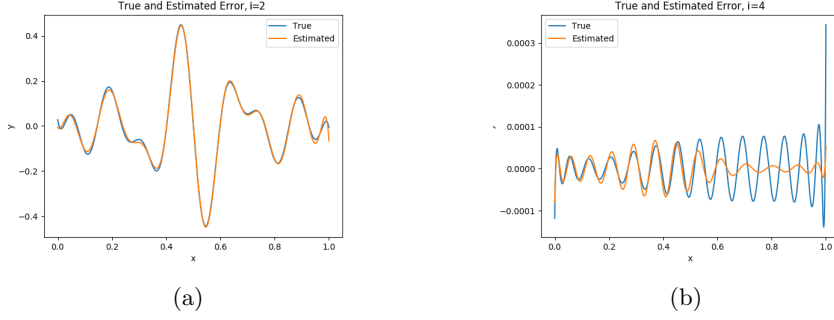


Fig. 2: (a) True error $u - u_{i-1}$ and approximate error φ_j^{NN} for $i = 2$. (b) True error $u - u_{i-1}$ and approximate error φ_j^{NN} for $i = 4$ with fixed width $n_i = 100$.

given $f \in L^2(\Omega)$, $\Omega = (0, 1)$, let $a(u, v) := (u, v)_{L^2(\Omega)}$ and $L(v) := (f, v)_{L^2(\Omega)}$ with f being the first four terms of the Fourier series for the square wave:

$$f(x) = \sin(x) + \frac{1}{3} \sin(3\pi x) + \frac{1}{5} \sin(5\pi x) + \frac{1}{7} \sin(7\pi x).$$

This is a simple function fitting problem whose exact solution is $u = f$. For this and all subsequent examples, we set $u_0 = 0$. The loss function is approximated by

$$\frac{L(v(\theta)) - a(u_0, v(\theta))}{\|v(\theta)\|} \approx \frac{\sum_{i=1}^{n_G} w_i [f(x_i)v(x_i; \theta) - u_0(x_i)v(x_i; \theta)]}{\sqrt{\sum_{i=1}^{n_G} w_i v(x_i; \theta)^2}}.$$

We use the hyperbolic tangent activation function $\sigma_i(t) = \tanh(\beta_i t)$, $\beta_i = 1 + 3(i - 1)$ at each Galerkin iteration and consider both the case when successive networks have fixed widths $n_i = 100$ for all i and the case when successive networks have increasing widths $n_i = 4 \times 2^{i-1}$. We set $\text{tol} = 10^{-6}$ and adaptively construct a Galerkin subspace that achieves an approximation with $\eta(u_{i-1}, \varphi_i^{NN}) < \text{tol}$. The hidden parameters are initialized such that $W_j^{(i)} = 1$ and $b_j^{(i)} = -jh$, $h = 1/n_i$ i.e. the biases are spaced uniformly throughout Ω . To evaluate the objective function and train the network,

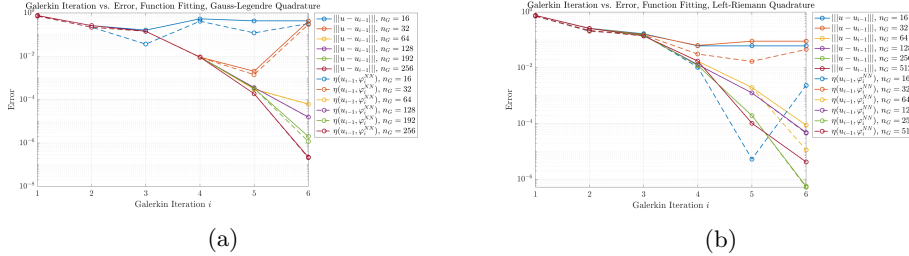


Fig. 3: (a) Error at each Galerkin iteration i using a Gauss-Legendre quadrature rule with varying number of nodes (b) the analogous results using a left Riemann-sum with varying number of nodes.

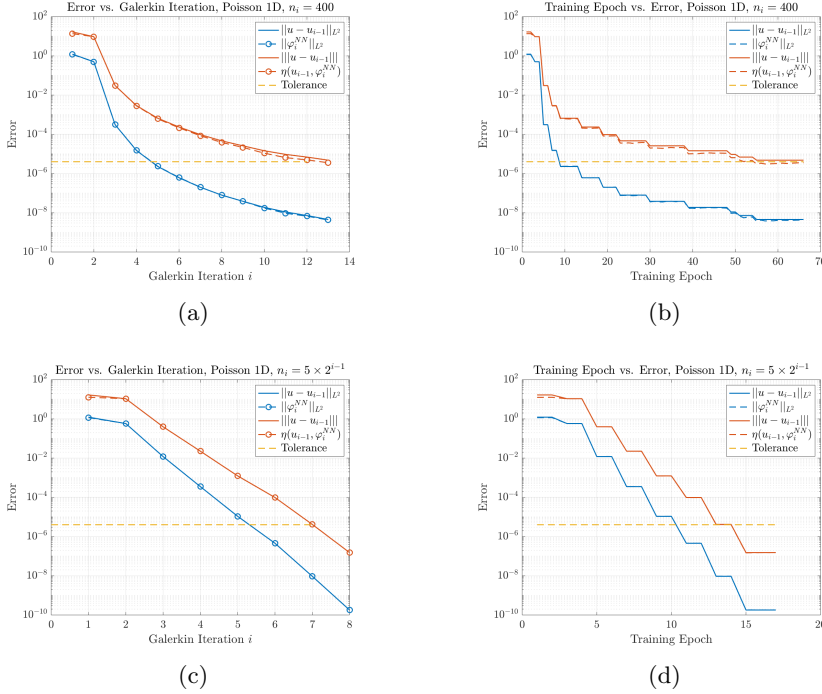


Fig. 4: Displacement of a string (Poisson equation in 1D). (a) Estimated and true error in the L^2 and energy norms at each Galerkin iteration, $n_i = 400$ for all i . (b) The piecewise constant segments (solid lines) denote the true errors for each Galerkin iteration i , while the dashed red line (resp. blue line) denotes the progress of the loss function (resp. L^2 error estimator $\|\varphi_i^{NN}\|_{L^2}$) in approximating the true errors within the each Galerkin iteration with $n_i = 400$. The x -axis thus denotes the cumulative training epoch over all Galerkin iterations. (c) and (d) The analogous results for $n_i = 5 \times 2^{i-1}$.

we employ a fixed Gauss-Legendre quadrature rule with 512 nodes to approximate all inner products. A separate Gauss-Legendre quadrature rule with 1000 nodes is used for validation, i.e. to compute the true errors.

Figure 1a shows the true L^2 error at each Galerkin iteration along with the estimator $\eta(u_{i-1}, \varphi_i^{NN})$ while Figure 1 shows the true and estimated L^2 error at each epoch. Figure 2 shows the true error $u - u_{i-1}$ and estimated error φ_i^{NN} for $i = 2$ and $i = 4$ with $n_i = 100$. It is apparent that initially, the low frequency components of the error are learned, with later iterations learning the high frequency error components. For $i = 2$, the low frequency error components are sufficiently learned by the network. However, for $i = 4$, the network lacks sufficient capacity to learn the high frequency error components, thus leading to inadequate training of the network and stagnation in the error. On the other hand, we observe from Figure 1 that there is no stagnation of the error in the later Galerkin iterations if n_i is increased with i . Moreover, the case when n_i is increased at each Galerkin iteration eventually achieves the same accuracy as the case when n_i is fixed at each Galerkin iteration while also achieving better computational efficiency due to utilizing initial networks with smaller widths.

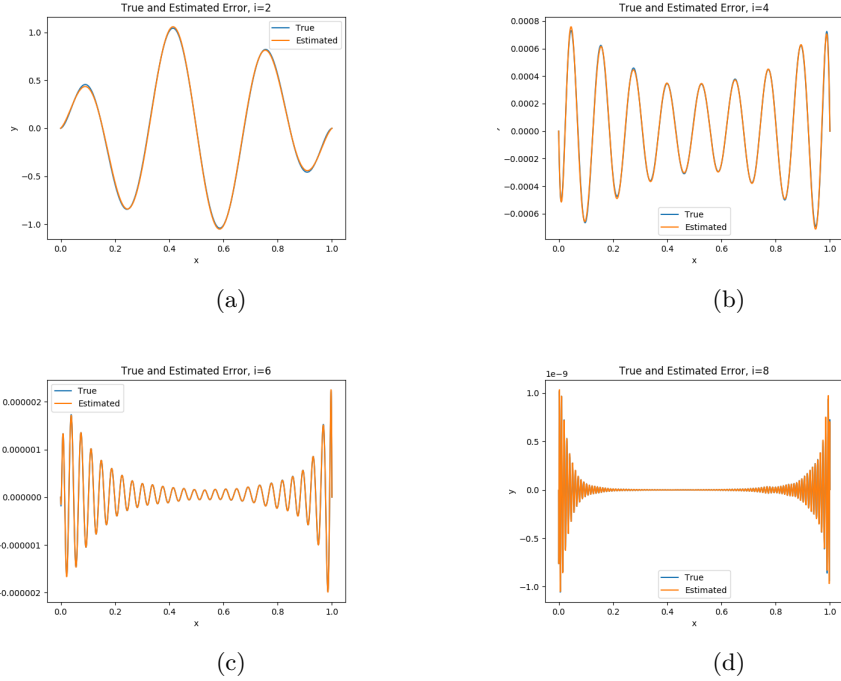


Fig. 5: Displacement of a string (Poisson equation in 1D). True error $u - u_{i-1}$ and estimated error φ_i^{NN} for $i = 2, 4, 6, 8$.

Of course, the quadrature rule used to approximate the loss function must be chosen sufficiently accurately. Figure 3 shows the convergence results obtained as the number of Gauss-Legendre quadrature points increases as well as a comparison with a left-Riemann sum quadrature rule. In each case, we observe that if the number of nodes is too small, the error either stagnates or increases eventually due to the inability of the quadrature rule to adequately evaluate the inner products in the loss function and (2.10) and (2.11).

3.2 Second Order Problems

3.2.1 Displacement of a String We now illustrate the approach for a simple linear ODE:

$$\begin{cases} -u'' = f, & \text{in } \Omega = (0, 1) \\ u + \varepsilon \partial_n u = 0, & \text{on } \partial\Omega, \end{cases}$$

where $\varepsilon > 0$ and $f(x) = (2\pi)^2 \sin(2\pi x) + (4\pi)^2 \sin(4\pi x) + (6\pi)^2 \sin(6\pi x)$, with f inducing a linear functional given by the rule $L(v) := (f, v)_\Omega$. The variational formulation is posed on the Hilbert space $X = H^1(\Omega)$ corresponding to the bilinear operator $a(u, v) = (u', v')_\Omega + \varepsilon^{-1}(u(0)v(0) + u(1)v(1))$. One can easily verify that a is symmetric and satisfies the conditions in (2.5). Observe that as $\varepsilon \rightarrow 0$, the derivative terms in the boundary condition vanish and we obtain $u(0) \rightarrow 0$ and $u(1) \rightarrow 0$, recovering the standard Poisson equation with homogeneous Dirichlet boundary conditions.

i	1	2	3	4	5	6	7	8	9	10
$\text{cond}(K^{(i)})$	1.00	1.00	1.00	1.00	1.02	1.03	1.07	1.08	1.09	1.18

Table 1: Displacement of a string. Condition number for the Galerkin matrix at each Galerkin iteration i .

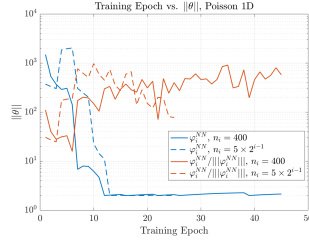


Fig. 6: Displacement of a string. The total norm of the network parameters for φ_i^{NN} and $\varphi_i^{NN} / \|\varphi_i^{NN}\|$.

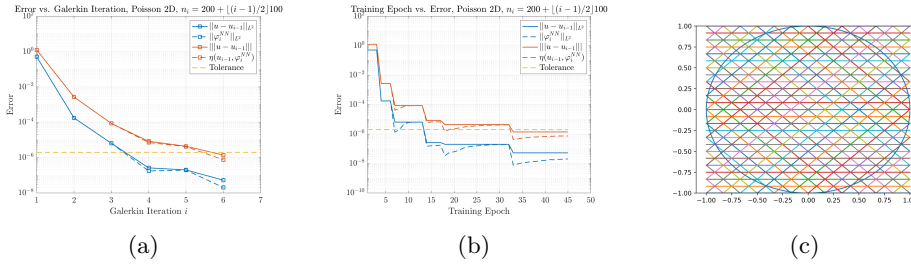


Fig. 7: Displacement of a membrane (Poisson equation in 2D). Estimated and exact error in the L^2 and energy norms at each Galerkin iteration (a) and epoch (b). Initial hyperplanes (c).

The parameter ε may thus be regarded as a penalization term which approximately enforces the homogeneous boundary condition $u(0) = u(1) = 0$. Alternatively, as $\varepsilon \rightarrow \infty$ we obtain $\partial_n u \rightarrow 0$ on $\partial\Omega$, and ε may be regarded as approximately imposing a homogeneous Neumann boundary condition. The true solution is

$$u(x) = \sin(2\pi x) + \sin(4\pi x) + \sin(6\pi x) + \frac{1}{1 + 2\varepsilon} (-24\pi\varepsilon x + 12\pi\varepsilon).$$

The corresponding loss function is approximated by

$$\frac{L(v(\theta)) - a(u_0, v(\theta))}{\|v(\theta)\|} \approx \frac{L_1 - L_2 - L_3}{\sqrt{\sum_{i=1}^{n_G} w_i v'(x_i; \theta)^2 + \varepsilon^{-1}(v(0; \theta)^2 + v(1; \theta)^2)}}$$

where $L_1 = \sum_{i=1}^{n_G} w_i f(x_i) v(x_i; \theta)$, $L_2 = \sum_{i=1}^{n_G} w_i u'_0(x_i) v'(x_i; \theta)$, and $L_3 = \varepsilon^{-1}[u_0(0) \cdot v(0; \theta) + u_0(1) v(1; \theta)]$.

The tolerance is set to $\text{tol} = 2 \times 10^{-6}$, and $\varepsilon = 10^{-4}$. The network architecture for Galerkin iteration i is as follows: $n_i = 400$, $\sigma_i(t) = \tanh(\beta_i t)$, $\beta_i = i$. The learning

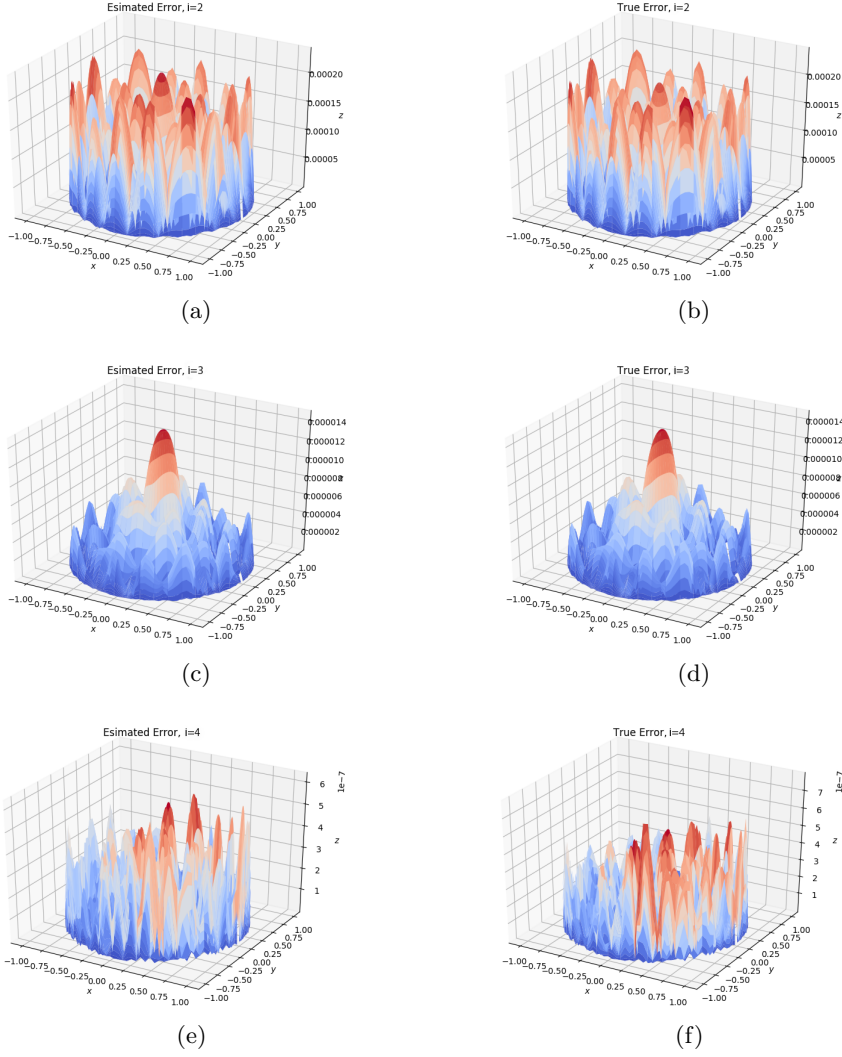


Fig. 8: Displacement of a membrane (Poisson equation in 2D). Exact error $u - u_{i-1}$ (right column) and approximate error φ_i^{NN} (left column) for $i = 2, 3, 4$.

rate is $\alpha = 2 \times 10^{-2}$. The hidden parameters are initialized in the same manner as in Section 3.1. For comparison, we shall also consider the set of network architectures given by $n_i = 5 \times 2^{i-1}$ and learning rate $\alpha = (2 \times 10^{-2})/1.1^{i-1}$. To evaluate the objective function and train the network, we employ a fixed Gauss-Legendre quadrature rule with 512 nodes to approximate all inner products. A separate Gauss-Legendre quadrature rule with 1000 nodes is used for validation.

Figure 4 shows the true errors $\|u - u_{i-1}\|_{L^2}$ and $\|u - u_{i-1}\|$ at the end of each Galerkin iteration as well as the corresponding error estimates $\|\varphi_i^{NN}\|_{L^2}$ and $\eta(u_{i-1}, \varphi_i^{NN})$. We also provide the analogous results after each training epoch. Figure 5 shows the exact error $u - u_{i-1}$ as well as the maximizer φ_i^{NN} at several stages of

i	1	2	3	4	5	6	7
$\text{cond}(K^{(i)})$	1.00	1.00	1.00	1.00	1.01	1.36	1.37

Table 2: Displacement of a membrane. Condition number for the Galerkin matrix at each Galerkin iteration i . We observe that $\text{cond}(A^{(i)}) = \mathcal{O}(1)$.

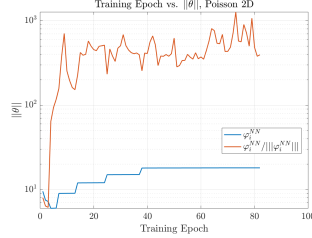


Fig. 9: Displacement of a membrane. The total norm of the network parameters for φ_i^{NN} and $\varphi_i^{NN} / \|\varphi_i^{NN}\|$.

the algorithm. We observe first that the initial Galerkin iterations reduce the error substantially, with further decreases beginning to stagnate as i grows larger whenever n_i is constant; stagnation is not an issue when n_i is increased with i . Moreover, both estimators $\eta(u_{i-1}, \varphi_i^{NN})$ and $\|\varphi_i^{NN}\|_{L^2}$ provide accurate estimates of the error, with negligible discrepancies beginning to show in the final Galerkin iterations. Figure 6 shows the total norm of the network parameters of φ_i^{NN} and $\varphi_i^{NN} / \|\varphi_i^{NN}\|$ at each training epoch. We observe that in both the normalized and unnormalized case, the network parameters are well-bounded and do not exhibit explosive behavior. Lastly, Table 1 shows the condition number of the matrix $K^{(j)}$ at each Galerkin iteration i . We observe that the condition number is approximately unity as expected.

3.2.2 Displacement of a Membrane We consider the Poisson equation in the unit disk:

$$\begin{cases} -\Delta u = f, & \text{in } \Omega = \{(x, y) : x^2 + y^2 < 1\} \\ u + \varepsilon \partial_n u = 0, & \text{on } \partial\Omega, \end{cases}$$

where, $f(x, y) = 2$. The variational formulation is posed on the Hilbert space $X = H^1(\Omega)$ corresponding to the bilinear operator $a(u, v) = (\nabla u, \nabla v)_\Omega + \varepsilon^{-1}(u, v)_{\partial\Omega}$ with data $L(v) := (f, v)_\Omega$. One can easily verify that a satisfies (2.5). The true solution is

$$u(x, y) = -\frac{x^2 + y^2}{2} + \varepsilon + \frac{1}{2}.$$

The corresponding loss function is approximated by

$$(3.1) \quad \frac{L_1 - L_2 - L_3}{\sqrt{\sum_{i=1}^{n_\Omega} w_i |\nabla v(x_i^\Omega; \theta)|^2 + \varepsilon^{-1} \sum_{i=1}^{n_{\partial\Omega}} w_i^{\partial\Omega} v(x_i^{\partial\Omega}; \theta)^2}}$$

where $L_1 = \sum_{i=1}^{n_\Omega} w_i^\Omega f(x_i) v(x_i; \theta)$, $L_2 = \sum_{i=1}^{n_\Omega} w_i^\Omega \nabla u_0(x_i^\Omega) \cdot \nabla v(x_i^\Omega; \theta)$, and $L_3 = \varepsilon^{-1} \sum_{i=1}^{n_{\partial\Omega}} w_i^{\partial\Omega} u_0(x_i^{\partial\Omega}) v(x_i^{\partial\Omega}; \theta)$. Here, $\{w^\Omega, x^\Omega\}$ is the quadrature rule in Ω while $\{w^{\partial\Omega}, x^{\partial\Omega}\}$ is the quadrature rule on $\partial\Omega$.

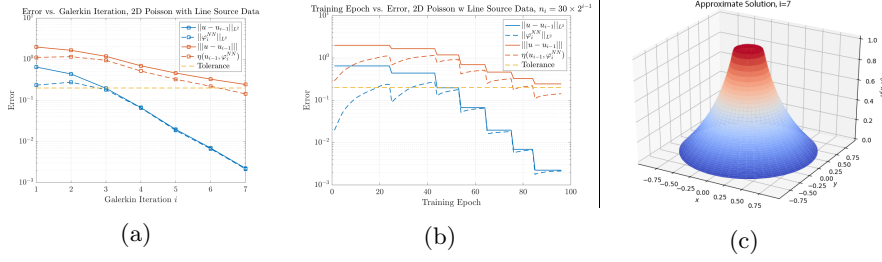


Fig. 10: Poisson equation with line source data, $R_e = 1 - 1/\pi^2$ and $R_0 = 1/\sqrt{29}$. (a) true and estimated errors after each Galerkin iteration (b) true and estimated errors after each training epoch (c) approximate solution u_i for $i = 7$.

The tolerance is set to $\text{tol} = 2 \times 10^{-6}$, and $\varepsilon = 10^{-4}$. The network architecture for Galerkin iteration i is as follows: $n_i = 200 + \lfloor \frac{i-1}{2} \rfloor \cdot 100$, $\sigma_i(t) = \tanh(t)$. The learning rate is $\alpha = (1 \times 10^{-2})/1.1^{i-1}$. The hidden parameters are initialized such that the hyperplanes lie parallel to $y = 0$, $x = 0$, $y = x$, or $y = -x$ as visualized in Figure 7 (right). To evaluate the loss function and train the network, we employ a fixed Gauss-Legendre quadrature rule with 128×128 nodes to approximate all inner products in the interior of the domain. A quadrature rule with 256 equally-spaced nodes is employed to approximate inner products on the boundary of the domain.

Figure 7 (left) shows the exact errors $\|u - u_{i-1}\|_{L^2}$ and $\|u - u_{i-1}\|$ at the end of each epoch along with the estimated errors $\|\varphi_i^{NN}\|_{L^2}$ and $\eta(u_{i-1}, \varphi_i^{NN})$ for our algorithm. Figure 8 shows the exact error $u - u_{i-1}$ (right column) as well as the computed maximizer φ_i^{NN} (left column) at several stages of our algorithm. We again observe good performance of the error estimator, with minor discrepancies beginning to show in the final Galerkin iteration. Figure 9 shows the total norm of the network parameters of φ_i^{NN} and $\|\varphi_i^{NN}\|/\|\varphi_i^{NN}\|$ at each training epoch, and we again observe well-boundedness of the parameters. Table 2 shows the condition number of the Galerkin matrix $K^{(i)}$ at Galerkin iteration i . We observe again that $\text{cond}(K^{(i)})$ is approximately unity.

3.2.3 Poisson Equation with Line Source Data We once more consider the Poisson equation in two dimensions, this time in the domain $\Omega = \{(x, y) : x^2 + y^2 < R_e^2\}$ with data $L : H^1(\Omega) \rightarrow \mathbb{R}$ defined by

$$L(v) := \int_{\Gamma} v \, ds, \quad \Gamma = \{(x, y) : x^2 + y^2 = R_0^2\}, \quad R_0 < R_e.$$

The exact variational solution is constant in the inner disk $\{(x, y) : x^2 + y^2 \leq R_0^2\}$ and logarithmic in the annulus $\Omega \setminus \{(x, y) : x^2 + y^2 \leq R_0^2\}$:

$$u(r, \theta) = -\frac{\varepsilon}{R_0 \log(R_0/R_e)} + \begin{cases} 1, & r \leq R_0 \\ \frac{1}{\log(R_0/R_e)} \log(r/R_e), & R_0 < r \leq R_e. \end{cases}$$

We consider two separate cases:

1. $R_e = 1 - 1/\pi^2$ and $R_0 = 1/\sqrt{29}$,
2. $R_e = 1 - 1/\pi^2$ and $R_0 = 7/(6\sqrt{2})$.

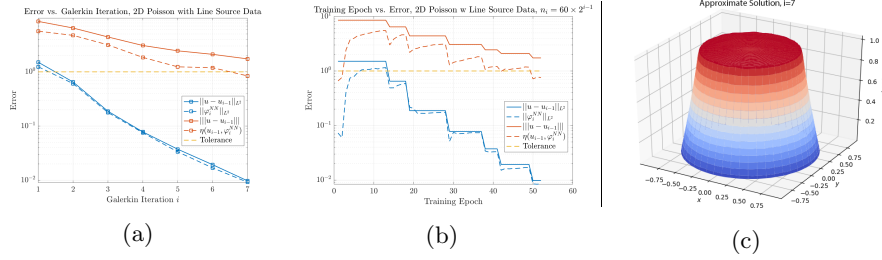


Fig. 11: Poisson equation with line source data, $R_e = 1 - 1/\pi^2$ and $R_0 = 7/(6\sqrt{2})$. (a) true and estimated errors after each Galerkin iteration (b) true and estimated errors after each training epoch (c) approximate solution u_i for $i = 7$.

In the first case, the logarithmic behavior dominates with a sharp cusp in the solution at $r = R_0$. In the second case, the solution still has a sharp cusp at $r = R_0$, but the logarithmic behavior is limited to the small annulus $R_0 \leq r \leq R_e$, which resembles a boundary layer. The corresponding loss function is approximated by

$$\frac{L_1 - L_2 - L_3}{\sqrt{\sum_{i=1}^{n_\Omega} w_i |\nabla v(x_i^\Omega; \theta)|^2 + \varepsilon^{-1} \sum_{i=1}^{n_{\partial\Omega}} w_i^{\partial\Omega} v(x_i^{\partial\Omega}; \theta)^2}}$$

where $L_1 = \sum_{i=1}^{n_\Gamma} w_i^\Gamma v(x_i^\Gamma; \theta)$, $L_2 = \sum_{i=1}^{n_\Omega} w_i^\Omega \nabla u_0(x_i^\Omega) \cdot \nabla v(x_i^\Omega; \theta)$, and $L_3 = \varepsilon^{-1} \cdot \sum_{i=1}^{n_{\partial\Omega}} w_i^{\partial\Omega} u_0(x_i^{\partial\Omega}) v(x_i^{\partial\Omega}; \theta)$. Here, $\{w^\Omega, x^\Omega\}$ is the quadrature rule in Ω , $\{w^{\partial\Omega}, x^{\partial\Omega}\}$ is the quadrature rule on $\partial\Omega$, and $\{w^\Gamma, x^\Gamma\}$ is the quadrature rule on Γ .

The tolerance is set to $\text{tol} = 2 \times 10^{-1}$ in the first case and $\text{tol} = 1.0$ in the second case, and $\varepsilon = 10^{-3}$. The network architecture for iteration i is as follows: $n_i = 30 \times 2^{i-1}$, $\sigma_i(t) = \tanh(\beta_i t)$, $\beta_i = i$. The learning rate for each basis function φ_i^{NN} is $\alpha_i = \frac{2 \times 10^{-2}}{1.1^{i-1}}$. The hidden parameters are initialized according to the box initialization detailed by Cyr, et. al. [4]. We employ fixed tensor-product Gauss-Legendre quadrature rule with 128×128 nodes in order to approximate inner products in the interior of the domain. We approximate the inner products on $\partial\Omega$ and Γ using 512 equally-spaced nodes on the circles of radii R_e and R_0 , respectively.

The true and estimated errors after each refinement and epoch are provided in Figure 10 along with a plot of the neural network approximation for case 1. The analogous results for case 2 are provided in Figure 11. Interestingly, the cusp along $r = R_0$ is resolved well in both cases without any encoding of the line source into the training data, albeit with a lower rate of convergence as compared with the examples with smooth solutions.

3.2.4 L-shaped Domain In this example, we consider the Poisson equation on an L-shaped domain in which the solution contains a corner singularity:

$$\begin{cases} -\Delta u = 1, & \text{in } \Omega = (-1, 1)^2 \setminus (-1, 0]^2 \\ u + \varepsilon \partial_n u = 0, & \text{on } \partial\Omega. \end{cases}$$

The loss function is given by (3.1) with $f \equiv 1$ and is approximated using the same methodology as in 3.2.2.

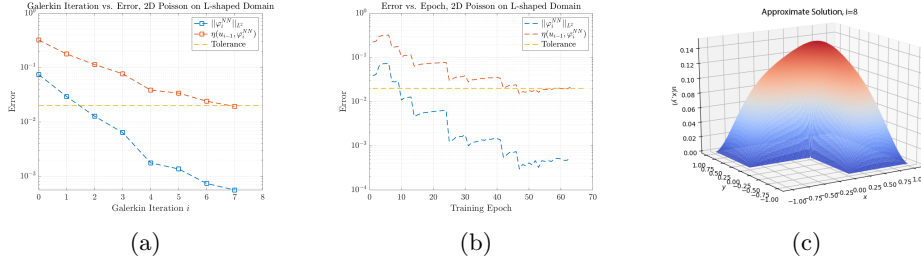


Fig. 12: Poisson equation in L-shaped domain. Estimated errors after each Galerkin iteration (a) and epoch (b) as well as approximate solution u_i for $i = 8$ (c).

The tolerance is set to $\text{tol} = 2 \times 10^{-2}$, and $\varepsilon = 10^{-4}$. The network architecture for iteration i is as follows: $n_i = 20 \times 2^{i-1}$, $\sigma_i(t) = \tanh(t)$. The learning rate for each basis function φ_i^{NN} is $\alpha_i = \frac{2 \times 10^{-2}}{1.1^{i-1}}$. The hidden parameters are again initialized according to the box initialization in $(-1, 1)^2$. We employ fixed Gauss-Legendre quadrature rules on each square subdomain of 128×128 nodes each in order to approximate inner products in the interior of the domain. A Gauss-Lobatto quadrature rule is employed on $[-1, 0] \times \{0\}$ and $\{0\} \times [-1, 0]$ to approximate the boundary containing the singularity, while Gauss-Legendre quadrature rules are employed on the remaining boundary edges.

Figure 12a shows the estimated errors $\|\varphi_i^{NN}\|_{L^2}$ and $\eta(u_{i-1}, \varphi_i^{NN})$ after each Galerkin iteration. Figure 12b shows the the estimated errors at each training iteration, while Figure 12c shows the approximate solution to the variational problem after eight Galerkin iterations. As expected, without a priori knowledge of the location of the corner singularity, we observe a reduced rate of convergence as compared to prior examples with smooth solutions. Nevertheless, our algorithm is capable of resolving the corner singularity.

3.3 Fourth Order Problems

3.3.1 Displacement of a Beam We consider the fourth-order ODE

$$\begin{cases} u^{(4)}(x) = f(x), & \text{in } \Omega = (0, 1) \\ u - \varepsilon_1 \partial_n(u'') = 0, & \text{on } \partial\Omega \\ u' + \varepsilon_2 \partial_n(u') = 0, & \text{on } \partial\Omega \end{cases}$$

with $f(x) = (2\pi)^4 \sin(2\pi x)$. The variational formulation is posed on the Hilbert space $X = H^2(\Omega)$ with corresponding bilinear operator $a(u, v) = (u'', v'')_{\Omega} + \varepsilon_1^{-1}(u(0)v(0) + u(1)v(1)) + \varepsilon_2^{-1}(u'(0)v'(0) + u'(1)v'(1))$ and data $L(v) = (f, v)_{\Omega}$. The exact solution is given by

$$u(x) = \sin(2\pi x) - 2\pi(2x - 1) \frac{4\varepsilon_1(\pi^2(6\varepsilon_2 - 2x^2 + 2x + 1) + 3) + x(x - 1)}{24\varepsilon_1 + 6\varepsilon_2 + 1}.$$

The corresponding loss function is approximated by

$$\frac{L_1 - L_2 - L_3 - L_4}{\sqrt{\sum_{i=1}^{n_G} w_i v''(x_i; \theta)^2 + \varepsilon_1^{-1}(v(0; \theta)^2 + v(1; \theta)^2) + \varepsilon_2^{-1}(v'(0; \theta)^2 + v'(1; \theta)^2)}}$$

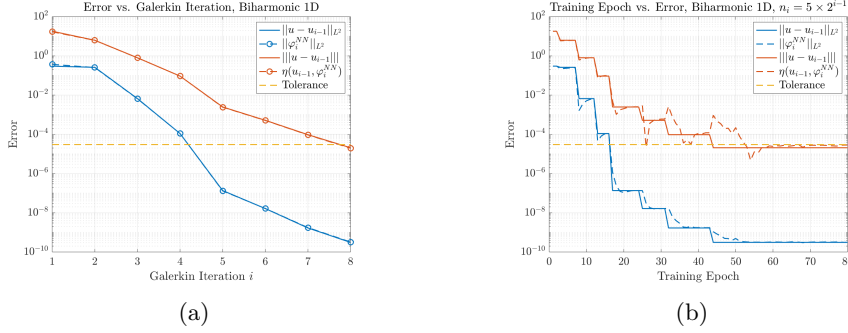


Fig. 13: The biharmonic equation in 1D. True and estimated error in the L^2 and energy norm at the end of each Galerkin iteration (a) and epoch (b).

where $L_1 = \sum_{i=1}^{n_G} w_i f(x_i) v(x_i; \theta)$, $L_2 = \sum_{i=1}^{n_G} w_i u_0''(x_i) v''(x_i; \theta)$, $L_3 = \varepsilon_1^{-1} [u_0(0) \cdot v(0; \theta) + u_0(1) v(1; \theta)]$, and $L_4 = \varepsilon_2^{-1} [u_0'(0) v'(0; \theta) + u_0'(1) v'(1; \theta)]$.

The tolerance is set to $\text{tol} = 3 \times 10^{-5}$, and $\varepsilon_1 = \varepsilon_2 = 10^{-4}$. The network architecture for iteration i is as follows: $n_i = 30 \times 2^{i-1}$, $\sigma_i(t) = \tanh(\beta_i t)$, $\beta_j = 1 + 3(j - 1)$. The learning rate for each basis function φ_i^{NN} is $\alpha_i = \frac{2 \times 10^{-2}}{1.1^{i-1}}$. The hidden parameters are initialized as in Section 3.1. To evaluate the loss function and train the network, we employ a fixed Gauss-Legendre quadrature rule with 512 nodes to approximate all inner products. A separate Gauss-Legendre quadrature rule with 1000 nodes is used for validation, i.e. to compute the exact errors in the L^2 and energy norms.

Figure 13a shows the exact errors $\|u - u_{i-1}\|_{L^2}$ and $\|u - u_{i-1}\|$ at the end of each Galerkin iteration along with the estimated errors $\|\varphi_i^{NN}\|_{L^2}$ and $\eta(u_{i-1}, \varphi_i^{NN})$ for our algorithm. Figure 13b shows the true and estimated errors at each training epoch, while Figure 14 shows the exact error $u - u_{i-1}$ as well as the maximizer φ_i^{NN} at several stages of refinement. We observe no difficulties in approximating both the true error and the true solution.

3.3.2 Beam with Applied Couple We consider the biharmonic equation with point moment source term:

$$\begin{cases} u^{(4)} = \delta'_{\{x=1/2\}}, & \text{in } \Omega = (0, 1) \\ u - \varepsilon_1 \partial_n(u'') = 0, & \text{on } \partial\Omega \\ u' + \varepsilon_2 \partial_n(u') = 0, & \text{on } \partial\Omega. \end{cases}$$

The bilinear operator a is as defined in Section 3.3.1 and $L(v) = -v'(1/2)$. The exact variational solution corresponding to $\varepsilon_1 = \varepsilon_2 = 0$ is

$$u(x) = \frac{1}{4}(x - 1/2)|x - 1/2| - \frac{1}{4}x^3 + \frac{3}{8}x^2 - \frac{1}{4}x + \frac{1}{16}.$$

The corresponding loss function is approximated by

$$\frac{L_1 - L_2 - L_3 - L_4}{\sqrt{\sum_{i=1}^{n_G} w_i v''(x_i; \theta)^2 + \varepsilon_1^{-1}(v(0; \theta)^2 + v(1; \theta)^2) + \varepsilon_2^{-1}(v'(0; \theta)^2 + v'(1; \theta)^2)}}$$

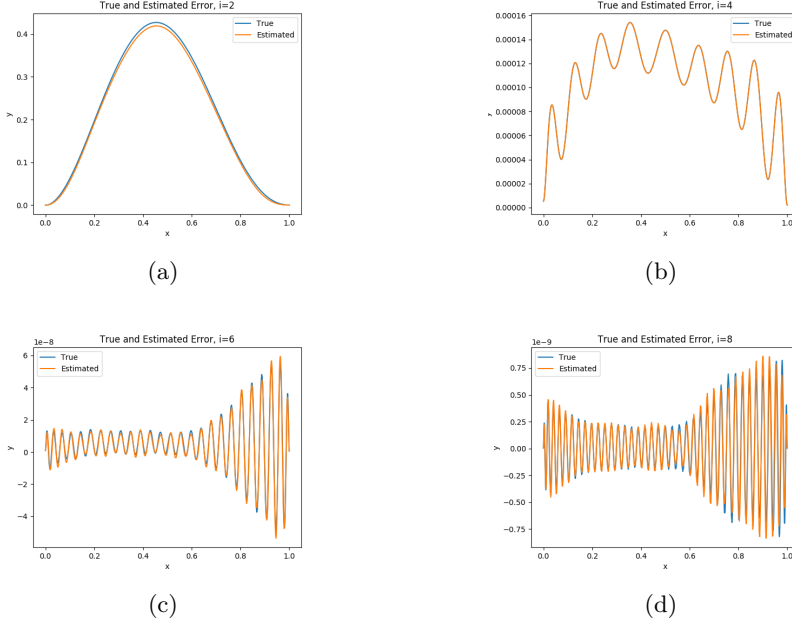


Fig. 14: Biharmonic equation. Exact error $u - u_{i-1}$ and approximate error φ_i^{NN} for $i = 2, 4, 6, 8$.

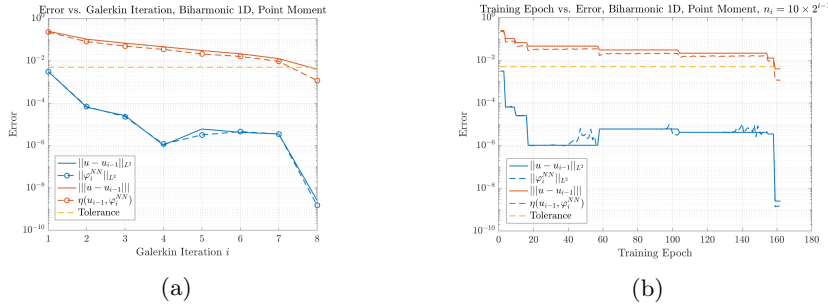


Fig. 15: The biharmonic equation in 1D with point moment. True and estimated error in the L^2 and energy norm at the end of each Galerkin iteration (a) and epoch (b).

where $L_1 = -v'(1/2; \theta)$, $L_2 = \sum_{i=1}^{n_G} w_i u_0''(x_i) v''(x_i; \theta)$, $L_3 = \varepsilon_1^{-1} [u_0(0)v(0; \theta) + u_0(1)v(1; \theta)]$, and $L_4 = \varepsilon_2^{-1} [u_0'(0)v'(0; \theta) + u_0'(1)v'(1; \theta)]$.

The tolerance is set to $\text{tol} = 4 \times 10^{-3}$, and $\varepsilon_1 = \varepsilon_2 = 10^{-5}$. The network architecture for iteration i is as follows: $n_i = 10 \times 2^{i-1}$, $\sigma_i(t) = \tanh(\beta_i t)$, $\beta_i = 1 + 3 \cdot 2^{i-1}$. The learning rate for each basis function φ_i^{NN} is $\alpha_i = \frac{1 \times 10^{-2}}{1.4^{i-1}}$. The hidden parameters are initialized as in Section 3.1. To evaluate the loss function and train the network, we employ a fixed Gauss-Legendre quadrature rule with 1024

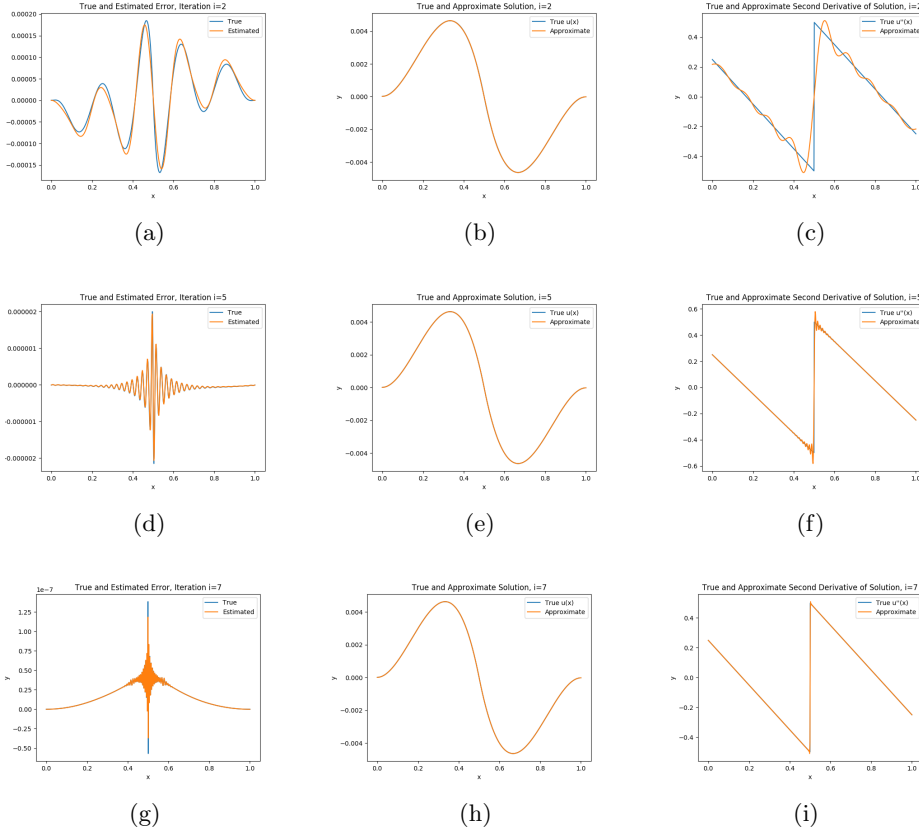


Fig. 16: Biharmonic equation with point moment in 1D. Exact error $u - u_{i-1}$ and approximate error φ_i^{NN} as well as numerical solution u_i and its derivative u_i'' for $i = 2$ (top row), $i = 5$ (middle row), and $i = 7$ (bottom row).

nodes to approximate all inner products. A separate Gauss-Legendre quadrature rule with 1000 nodes is used for validation, i.e. to compute the exact errors in the L^2 and energy norms.

Figure 15a shows the true errors $\|u - u_{i-1}\|_{L^2}$ and $\|\varphi_i^{NN}\|_{L^2}$ at the end of each Galerkin iteration along with the estimated errors $\eta(u_{i-1}, \varphi_i^{NN})$ for our algorithm. Figure 15b shows the true and estimated errors at each training epoch, while Figure 16 shows the exact error $u - u_{i-1}$ as well as the maximizer φ_i^{NN} at several stages of refinement along with both the numerical solution u_i and its second derivative u_i'' . We observe that initially, low frequency oscillations in the error are learned followed later by suppression of the high frequency error components which are particularly notable near the discontinuity in the second derivative of u_i .

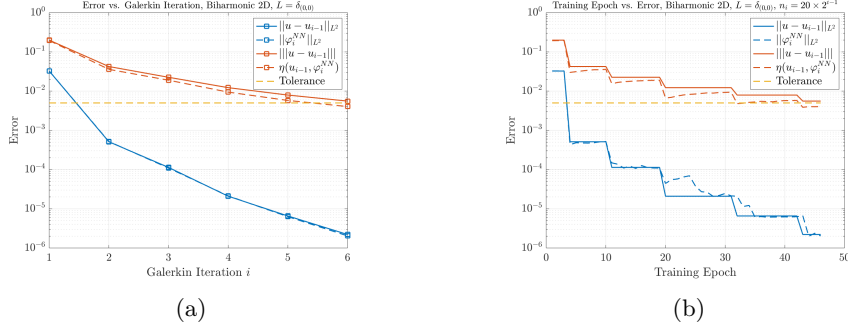


Fig. 17: The biharmonic equation in 2D. True and estimated error in the L^2 and energy norm at the end of each Galerkin iteration (a) and epoch (b).

3.3.3 Circular Plate with Point Load We consider the two-dimensional biharmonic equation with point load source term in the unit disk:

$$\begin{cases} \Delta^2 u = \delta_{\{(0,0)\}} & \text{in } \Omega = \{(x, y) : x^2 + y^2 < 1\} \\ u - \varepsilon_1 \partial_n (\Delta u) = 0 & \text{on } \partial\Omega \\ \Delta u + \varepsilon_2 \partial_n u = 0 & \text{on } \partial\Omega. \end{cases}$$

The variational formulation is again posed on $X = H^2(\Omega)$ with bilinear operator $a(u, v) = (\Delta u, \Delta v)_\Omega + \varepsilon_1^{-1} (u, v)_{\partial\Omega} + \varepsilon_2 (\partial_n u, \partial_n v)_{\partial\Omega}$ and data $L(v) = v(0, 0)$. The exact variational solution is given by

$$u(r, \theta) = \frac{r^2}{8\pi} \log(r) + c_1 r^2 + c_2, \quad c_1 = \frac{1}{4 + 2\varepsilon_2} \cdot \left(-\frac{\varepsilon_2}{2\pi} - \frac{1}{8\pi}\right), \quad c_2 = -c_1 + \frac{\varepsilon_1}{2\pi}.$$

The corresponding loss function is approximated by

$$\frac{L_1 - L_2 - L_3 - L_4}{\sqrt{\sum_{i=1}^{n_\Omega} w_i |\Delta v(x_i^\Omega; \theta)|^2 + \varepsilon^{-1} \sum_{i=1}^{n_{\partial\Omega}} w_i^{\partial\Omega} v(x_i^{\partial\Omega}; \theta)^2 + \varepsilon_2 \sum_{i=1}^{n_{\partial\Omega}} w_i^{\partial\Omega} \partial_n v(x_i^{\partial\Omega}; \theta)^2}}$$

where $L_1 = v(0; \theta)$, $L_2 = \sum_{i=1}^{n_\Omega} w_i^\Omega \Delta u_0(x_i^\Omega) \Delta v(x_i^\Omega; \theta)$, $L_3 = \varepsilon_1^{-1} \sum_{i=1}^{n_{\partial\Omega}} w_i^{\partial\Omega} u_0(x_i^{\partial\Omega}) \cdot v(x_i^{\partial\Omega}; \theta)$, and $L_4 = \varepsilon_2 \sum_{i=1}^{n_{\partial\Omega}} w_i^{\partial\Omega} \partial_n u_0(x_i^{\partial\Omega}) \partial_n v(x_i^{\partial\Omega}; \theta)$. Here, $\{w_i^\Omega, x_i^\Omega\}$ is the quadrature rule in Ω while $\{w_i^{\partial\Omega}, x_i^{\partial\Omega}\}$ is the quadrature rule on $\partial\Omega$.

The tolerance is set to $\text{tol} = 5 \times 10^{-3}$, and $\varepsilon_1 = \varepsilon_2 = 10^{-5}$. The network architecture for iteration i is as follows: $n_i = 20 \times 2^{i-1}$, $\sigma_i(t) = \tanh(t)$. The learning rate for each basis function φ_i is $\alpha_i = \frac{1 \times 10^{-2}}{1.1^{i-1}}$. The hidden parameters are initialized according to the box initialization in [4]. We employ fixed tensor product Gauss-Legendre quadrature rule with 100×100 nodes in order to approximate inner products in the interior of the domain. We approximate the inner products on $\partial\Omega$ using 256 equally-spaced nodes on $\partial\Omega$.

Figure 17a shows the true errors $\|u - u_{i-1}\|_{L^2}$ and $\|u - u_{i-1}\|$ at the end of each Galerkin iteration along with the estimated errors $\|\varphi_i^{NN}\|_{L^2}$ and $\eta(u_{i-1}, \varphi_i^{NN})$ for our algorithm. Figure 17b shows the true and estimated errors at each training epoch, while Figure 18 shows the true error $u - u_i$ (middle column) as well as the

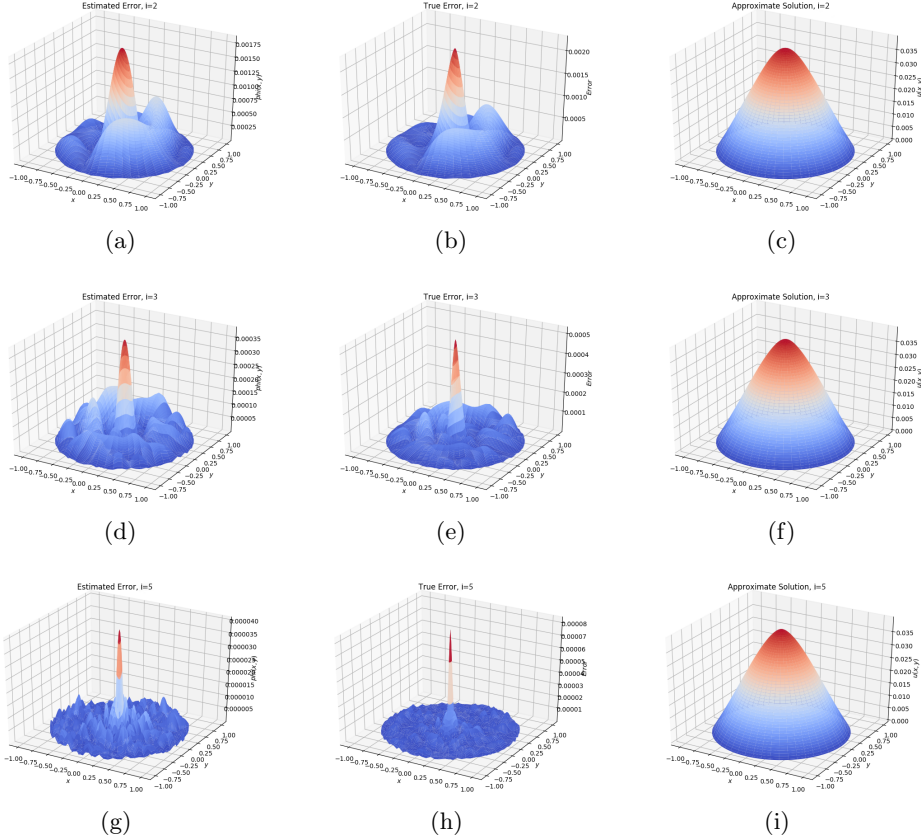


Fig. 18: Biharmonic equation in 2D with point load source. True error $u - u_{i-1}$ (middle column) and estimated error φ_i^{NN} (left column) as well as numerical solution u_i (right column) for $i = 2, 3, 5$.

maximizer φ_i^{NN} (left column) and approximate solution u_i (right column) at several stages of refinement. We observe no difficulties in handling the singular data in two dimensions.

4 Conclusions We have introduced a framework for adaptively generating basis functions for a finite-dimensional subspace which may be used in a standard Galerkin method for approximating variational problems. We have demonstrated that each basis function φ_i^{NN} may be expressed as the realization of a neural network $V_{n_i, C_i}^{\sigma_i}$ with a single hidden layer by learning the dual representation of the weak residual $r(u_{i-1}) : X \rightarrow \mathbb{R}$. Furthermore, we have shown that $\eta(u_{i-1}, \varphi_i^{NN})$ is an equivalent measure of the error $\|u - u_{i-1}\|$ and constitutes a robust a posteriori error estimate. We emphasize that our algorithm may be applied seamlessly to the broad class of problems in this section with no major modifications. This is in contrast to e.g. the finite element method which requires a tailored approach depending on the underlying Sobolev space and spatial dimension of the variational problem.

5 Acknowledgments This material is based upon work supported by the National Science Foundation Graduate Research Fellowship under Grant No. 1644760 as well as PhILMS grant DE-SC0019453.

REFERENCES

- [1] J. BERG AND K. NYSTRÖM, *A unified deep artificial neural network approach to partial differential equations in complex geometries*, *Neurocomputing*, 317 (2018), pp. 28–41.
- [2] S. BRENNER AND R. SCOTT, *The mathematical theory of finite element methods*, vol. 15, Springer Science & Business Media, 2007.
- [3] G. CYBENKO, *Approximation by superpositions of a sigmoidal function*, *Mathematics of control, signals and systems*, 2 (1989), pp. 303–314.
- [4] E. C. CYR, M. A. GULIAN, R. G. PATEL, M. PEREGO, AND N. A. TRASK, *Robust training and initialization of deep neural networks: An adaptive basis viewpoint*, arXiv preprint arXiv:1912.04862, (2019).
- [5] P. J. DAVIS AND P. RABINOWITZ, *Methods of numerical integration*, Courier Corporation, 2007.
- [6] M. DISSANAYAKE AND N. PHAN-THIEN, *Neural-network-based approximations for solving partial differential equations*, *communications in Numerical Methods in Engineering*, 10 (1994), pp. 195–201.
- [7] A. ERN AND J.-L. GUERMOND, *Theory and practice of finite elements*, vol. 159, Springer Science & Business Media, 2013.
- [8] G. B. FOLLAND, *Real analysis: modern techniques and their applications*, vol. 40, John Wiley & Sons, 1999.
- [9] S. GERSCHGORIN, *Über die abgrenzung der eigenwerte einer matrix*, *Izvestija Akademii Nauk SSSR, Serija Matematika*, 7 (1931), pp. 749–754.
- [10] J. HAN, A. JENTZEN, AND E. WEINAN, *Solving high-dimensional partial differential equations using deep learning*, *Proceedings of the National Academy of Sciences*, 115 (2018), pp. 8505–8510.
- [11] J. HE, L. LI, J. XU, AND C. ZHENG, *Relu deep neural networks and linear finite elements*, *Journal of Computational Mathematics*, (2019).
- [12] K. HORNIK, *Approximation capabilities of multilayer feedforward networks*, *Neural networks*, 4 (1991), pp. 251–257.
- [13] A. D. JAGTAP, K. KAWAGUCHI, AND G. E. KARNIADAKIS, *Adaptive activation functions accelerate convergence in deep and physics-informed neural networks*, *Journal of Computational Physics*, 404 (2020), p. 109136.
- [14] E. KHARAZMI, Z. ZHANG, AND G. KARNIADAKIS, *Variational physics-informed neural networks for solving partial differential equations*, arXiv preprint arXiv:1912.00873, (2019).
- [15] D. P. KINGMA AND J. BA, *Adam: A method for stochastic optimization*, arXiv preprint arXiv:1412.6980, (2014).
- [16] I. E. LAGARIS, A. LIKAS, AND D. I. FOTIADIS, *Artificial neural networks for solving ordinary and partial differential equations*, *IEEE transactions on neural networks*, 9 (1998), pp. 987–1000.
- [17] I. E. LAGARIS, A. C. LIKAS, AND D. G. PAPAGEORGIOU, *Neural-network methods for boundary value problems with irregular boundaries*, *IEEE Transactions on Neural Networks*, 11 (2000), pp. 1041–1049.
- [18] M. LESHNO, V. Y. LIN, A. PINKUS, AND S. SCHOCKEN, *Multilayer feedforward networks with a nonpolynomial activation function can approximate any function*, *Neural networks*, 6 (1993), pp. 861–867.
- [19] S. MISHRA AND R. MOLINARO, *Estimates on the generalization error of physics informed neural networks (pinns) for approximating pdes ii: A class of inverse problems*, arXiv preprint arXiv:2007.01138, (2020).
- [20] P. PETERSEN, M. RASLAN, AND F. VOIGTLAENDER, *Topological properties of the set of functions generated by neural networks of fixed size*.
- [21] M. RAISSI, P. PERDIKARIS, AND G. E. KARNIADAKIS, *Physics-informed neural networks: A deep learning framework for solving forward and inverse problems involving nonlinear partial differential equations*, *Journal of Computational Physics*, 378 (2019), pp. 686–707.
- [22] J. SIRIGNANO AND K. SPILIOPOULOS, *Dgm: A deep learning algorithm for solving partial differential equations*, *Journal of computational physics*, 375 (2018), pp. 1339–1364.
- [23] E. WEINAN AND B. YU, *The deep ritz method: a deep learning-based numerical algorithm for solving variational problems*, *Communications in Mathematics and Statistics*, 6 (2018), pp. 1–12.

- [24] Y. ZANG, G. BAO, X. YE, AND H. ZHOU, *Weak adversarial networks for high-dimensional partial differential equations*, Journal of Computational Physics, (2020), p. 109409.